The EMBO Journal Vol.18 No.20 pp.5761–5777, 1999

The RNA export factor Gle1p is located on the cytoplasmic fibrils of the NPC and physically interacts with the FG-nucleoporin Rip1p, the DEAD-box protein Rat8p/Dbp5p and a new protein Ymr255p

Yvan Strahm, Birthe Fahrenkrog[1], Daniel Zenklusen, Elizabeth Rychner, Julia Kantor[2], Michael Rosbash[2] and Françoise Stutz[3]

Microbiology Institute, CHUV, Bugnon 44, 1011 Lausanne, [1]M.E.Müller Institute for Structural Biology, Biozentrum, University of Basel, CH-4056 Basel, Switzerland and [2]Howard Hughes Medical Institute, Biology Department, Brandeis University, Waltham, MA 02254, USA

[3]Corresponding author
e-mail: fstutz@hola.hospvd.ch

Y.Strahm and B.Fahrenkrog contributed equally to this work

Gle1p is an essential, nuclear pore complex (NPC)-associated RNA export factor. In a screen for high copy suppressors of a *GLE1* mutant strain, we identified the FG-nucleoporin Rip1p and the DEAD-box protein Rat8p/Dbp5p, both of which have roles in RNA export; we also found Ymr255p/Gfd1p, a novel inessential protein. All three high copy suppressors interact with the C-terminal domain of Gle1p; immunoelectron microscopy localizations indicate that Gle1p, Rip1p and Rat8p/Dbp5p are present on the NPC cytoplasmic fibrils; Rip1p was also found within the nucleoplasm and on the nuclear baskets. *In vivo* localizations support the hypothesis that Rip1p contributes to the association of Gle1p with the pore and that Gle1p, in turn, provides a binding site for Rat8p/Dbp5p at the NPC. These data are consistent with the view that Gle1p, Rip1p, Rat8p/Dbp5p and Ymr255p/Gfd1p associate on the cytoplasmic side of the NPC to act in a terminal step of RNA export. We also describe a human functional homologue of Rip1p, called hCG1, which rescues Rip1p function in yeast, consistent with the evolutionary conservation of this NPC-associated protein.

Keywords: DEAD-box protein/FG-nucleoporin/nuclear pore complex/RNA export/yeast

Introduction

Transport through nuclear pores requires a concerted interaction between the structural components of the nuclear pore complex (NPC) and the soluble transport factors that bind specific cargoes and shuttle between the nuclear and cytoplasmic compartments. Transport is a signal-mediated and energy-dependent process. Localization signals within the transported cargoes are recognized by transport receptors, which mediate either import or export. These receptors (importins or exportins) are members of a family of proteins related to the import receptor importin-β. They all share the functional characteristic of binding to phenylalanine–glycine (FG) repeat domains of a family of NPC proteins called FG-nucleoporins, as well as the small GTPase Ran/Gsp1p (reviewed in Mattaj and Englmeier, 1998). Ran acts as a molecular switch that regulates the association of transport receptors with their cargoes (reviewed in Dahlberg and Lund, 1998). The first transport receptor identified was importin-β, the import factor for nuclear proteins containing a 'classical' nuclear localization signal (NLS) (reviewed in Görlich, 1998).

Export receptors were identified more recently, and a major contributor to the understanding of export was the human immunodeficiency virus type 1 (HIV-1) Rev protein. Rev is a shuttling RNA-binding protein whose role is to promote the export of partially spliced or unspliced viral transcripts. Rev was the first protein in which a nuclear export signal (NES) was identified. Rev-NES was shown to function in a variety of organisms including yeast, indicating that the export machinery targeted by Rev was evolutionarily conserved (reviewed in Pollard and Malim, 1998). A yeast two-hybrid screen initially identified the yeast FG-nucleoporin Rip1p and the non-homologous mammalian protein hRip/RAB as potential targets for Rev-NES at the nuclear pore (Bogerd *et al*., 1995; Fritz *et al*., 1995; Stutz *et al*., 1995). However, the export factor Crm1/Xpo1p was subsequently shown to interact directly with Rev-NES in a Ran-GTP-dependent manner and to promote the export of Rev and its associated RNA, presumably through an interaction with components of the NPC (reviewed in Mattaj and Englmeier, 1998; Stutz and Rosbash, 1998). As the initially described Rev–Rip1p two-hybrid interaction was compromised in a *CRM1* mutant background, it was proposed that Crm1p bridges this association; Crm1p interacts with Rip1p *in vitro* (Floer and Blobel, 1999) but also with many other FG-repeat domains in the two-hybrid assay (Neville *et al*., 1997). However, most of these domains can be deleted individually without affecting viability (Fabre and Hurt, 1997), indicating extensive functional redundancy, and it is unclear at present which FG-repeat regions are relevant to Crm1p function *in vivo*.

Despite the identification of Crm1p and the elucidation of its role in Rev-mediated RNA export, our understanding of cellular RNA export is still limited. Newly synthesized RNAs are exported as ribonucleoprotein complexes (RNPs), which harbour multiple signals recognized by the export machinery. The export of the different classes of RNAs is dependent on nuclear Ran-GTP, suggesting the involvement of exportins in these processes (Izaurralde *et al*., 1997). There is strong evidence that Crm1p exports UsnRNAs and 5S RNAs in vertebrate systems, but the exact contribution of Crm1p to mRNA export is still under debate (Neville and Rosbash, 1999; reviewed in Stutz and Rosbash, 1998).

Several shuttling hnRNP proteins (hnRNPA1, hnRNPK)

or the yeast hnRNP-like proteins, Npl3p and Hrp1p/Nab4p, have been proposed to participate in mRNA export (reviewed in Nakielny *et al*., 1997; Izaurralde and Adam, 1998; Stutz and Rosbash, 1998). However, no clear physical connection has yet been established between these RNA-binding proteins and a specific export factor or component of the NPC.

The understanding of RNP translocation through the nuclear pore relies in part on the functional characterization of the NPC components involved in that process. Numerous nucleoporins have been identifed in yeast, a number of which assemble in discrete NPC sub-complexes. The potential role of these sub-complexes has been elucidated mainly by determining how deletion or mutation of individual members affect NPC function (e.g. RNA export, protein import) or biogenesis (reviewed in Doye and Hurt, 1997; Fabre and Hurt, 1997). Nup159p and Nup84p define two sub-complexes with primary roles in RNA export (Siniossoglou *et al*., 1996; Teixeira *et al*., 1997; Belgareh *et al*., 1998; Hurwitz *et al*., 1998; and see Discussion).

Several additional factors essential for poly(A)$^+$ RNA export have been found in association with the NPC. One consists of the yeast Mex67p/Mtr2p protein complex; the two proteins are present on both sides of the NPC, suggesting that their localization may be dynamic (Santos-Rosa *et al*., 1998). TAP, the human homologue of Mex67p, is the cellular factor recruited by the CTE (constitutive transport element) of type D retroviruses to export unspliced viral RNAs (Grüter *et al*., 1998). TAP shuttles between nucleus and cytoplasm, and both Mex67p and TAP bind RNA and interact with FG-nucleoporins (Katahira *et al*., 1999). TAP and Mex67p may promote mRNA export by mediating the interaction of mRNPs with FG-nucleoporins at the pore. These properties define TAP and Mex67p as new types of export receptors, not related to the importin-β family of transporters (de Castillia and Rout, 1999).

The DEAD-box protein Rat8p/Dbp5p is also an essential player in mRNA export. Rat8p/Dpb5p was detected in the cytoplasm as well as in association with NPCs. The RNA-dependent ATPase and ATP-dependent RNA-unwinding activities of Rat8p/Dpb5p were proposed to participate in RNA export by restructuring RNP complexes during translocation through and release from the NPC. In the cytoplasm, the energy generated by ATP hydrolysis may also be used to dissociate shuttling RNA-binding proteins and promote their recycling back into the nucleus (Snay-Hodge *et al*., 1998; Tseng *et al*., 1998; Schmitt *et al*., 1999).

Finally, Gle1p is another NPC-associated component essential for RNA export; it was identified initially in a screen for mutations synthetically lethal with a *NUP100* disruption (Murphy and Wente, 1996) and as a high copy suppressor of the *rat7-1/nup159-1* temperature-sensitive allele (Del Priore *et al*., 1996). Gle1p was also found in a screen for cold-sensitive mutants exhibiting a poly(A)$^+$ RNA export defect (Noble and Guthrie, 1996) and in a *ΔRIP1* synthetic lethal screen (Stutz *et al*., 1997); additional genetic interactions have been described between Gle1p and NPC or NPC-associated components, most of which have a defined role in RNA export (Snay-Hodge *et al*., 1998). Gle1p was proposed to contain a Rev-like NES essential for poly(A)$^+$ RNA export. In support of a connection with the NES export pathway, Gle1p was shown to interact with Rip1p in two-hybrid and *in vitro* assays and proposed to promote poly(A)$^+$ RNA export in a process similar to Rev-mediated RNA export (Murphy and Wente, 1996). There is no evidence, however, that Gle1p shuttles or binds RNA.

Our studies on Rip1p and Gle1p have pointed to a different functional relationship between these two proteins. We isolated *GLE1* alleles in a screen for mutations synthetically lethal with a *RIP1* deletion, supporting a role for Rip1p in poly(A)$^+$ RNA export. Rip1p contains two domains: an N-terminal FG-repeat region, which interacts with Crm1p and Rev (presumably through bridging by Crm1p) in the two-hybrid assay (Neville *et al*., 1997), and a unique C-terminus (referred to as the C-domain). The C-domain is sufficient to rescue synthetic lethality of *GLE1* mutants, indicating a functional interaction between this region and Gle1p. Rip1p also becomes essential under heat shock conditions, where it is required for the efficient export of heat-induced transcripts; the short C-domain of Rip1p is both necessary and sufficient for this activity (Saavedra *et al*., 1997; Stutz *et al*., 1997). These data suggest that the C-domain of Rip1p performs a similar function in RNA export under stress or normal conditions.

Here we further characterize the functional relationship between Gle1p and Rip1p and show that the physical interaction between these two proteins is distinct from the Rev–Rip1p interaction. Through a high copy suppressor screen of a *GLE1* mutant strain, we identified Rip1p and two additional Gle1p partners: the DEAD-box protein Rat8p/Dbp5p and an unknown protein, Ymr255p. Immunoelectron microscopy localizations indicate that these interactions are likely to take place on the cytoplasmic side of the NPC and may therefore contribute to a late step of RNA export. We also describe the identification of a human homologue of Rip1p, termed hCG1, which recapitulates several aspects of Rip1p function in yeast.

Results

hCG1, the human homologue of Rip1p/Nup42p

As earlier data implicated Rip1p in RNA export, we asked whether this protein was evolutionarily conserved. Given the functional importance of the Rip1p unique C-terminus (Stutz *et al*., 1997), database searches were performed with the 66 C-terminal residues. A single sequence was identified (DDBJ/EMBL/GenBank accession No. U97198), corresponding to a complete human cDNA of 1778 bp named hCG1, previously described in an unrelated approach (Van Laer *et al*., 1997). hCG1 mRNA encodes a 423 amino acid protein. ClustalW alignment of the Rip1p and hCG1 proteins revealed a 55% homology over the entire length and a 35% identity over the C-terminal 40 amino acids. These data indicated a significant conservation of the region important for Rip1p function (Figure 1A). hCG1 also contains multiple FG-dipeptides in its N-terminal domain and therefore presents a domain organization similar to that of Rip1p. These observations together with the functional data presented below support that hCG1 corresponds to the human homologue of Rip1p/Nup42p. Further BLAST searches identified several mouse expressed sequence tags (ESTs) encoding a protein with

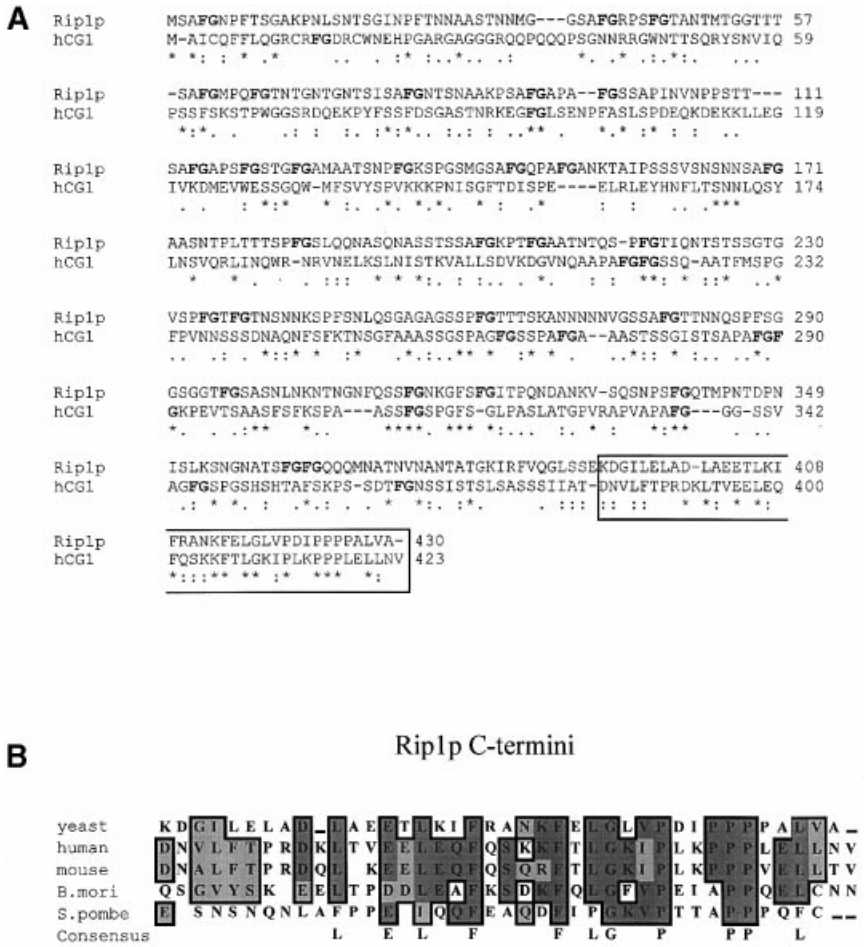

Fig. 1. The functional homologues of Rip1p/Nup42p are mostly conserved in the C-terminal domain. (**A**) Sequence comparison of Rip1p and hCG1. ClustalW sequence alignment revealed 20% perfect matches (*), 15% high similarity (:) and 20% low similarity (.) residues. The boxed region highlights the 40 highly conserved C-terminal amino acids (35% identity, 30% high similarity). The FG-dipeptides scattered through the N-terminal domains of Rip1p and hCG1 are indicated in bold. (**B**) ClustalW multiple alignment of the C-terminal domains from Rip1p, hCG1, and putative mouse, *S.pombe* and *B.mori* homologues. Identical and similar residues are shown in dark and light grey boxes, respectively. The derived consensus sequence corresponds to residues identical in at least four species.

extensive homology to hCG1; finally, *Bombyx mori* and *Schizosaccharomyces pombe* sequences were identified with C-terminal domains highly related to the corresponding region in Rip1p/hCG1 (Figure 1B). The comparison of the Rip1p C-terminal domains revealed a series of highly conserved residues with a spacing strictly maintained among the five species. While this manuscript was in preparation, hCG1 was also identified in two-hybrid screens with the human TAP and HIV-1 Rev proteins (Farjot *et al*., 1999; Katahira *et al*., 1999).

hCG1 can substitute for Rip1p function in yeast

Rip1p is not essential under normal growth conditions but is required under heat shock for the efficient export of heat-induced transcripts. Rip1p also becomes essential in the presence of mutations in the RNA export factor Gle1p, indicating a contribution of Rip1p to non-heat shock RNA export. Earlier work showed that the unique C-domain of Rip1p was sufficient to restore heat shock RNA export at 42°C in a *ΔRIP1* strain and to rescue synthetic lethality in *GLE1* mutant strains (Stutz *et al*., 1997). To test whether hCG1 was functionally homologous to Rip1p, we examined the ability of its C-terminal domain to rescue Rip1p function. For this purpose, the C-terminal regions of Rip1p and hCG1 were expressed in yeast as LexA fusions by cloning into the two-hybrid bait vector pEG202 (HIS3, 2μ). Fusion to LexA allowed good expression of these short peptides when assayed by Western blotting (data not shown), and the same fusions were used in two-hybrid interaction assays (see below).

First, we tested whether the LexA fusions restored heat shock RNA export at 42°C in a *ΔRIP1* strain. Heat shock protein synthesis at 42°C was used as an assay for heat shock RNA export (Figure 2A). For comparison, [^{35}S]methionine incorporation at 25 or 42°C was monitored in a W303 wild-type strain in which heat shock proteins are strongly induced at 42°C (Figure 2A, lanes 1 and 2). In contrast, no heat shock proteins were synthesized at 42°C in a *ΔRIP1* strain transformed with an empty vector, due to the potent block of heat shock RNA export in the absence of Rip1p (compare lanes 2 and 4); heat shock protein synthesis was restored in *ΔRIP1* with a plasmid expressing wild-type Rip1p (RIP1; lane 5). More importantly, heat shock protein synthesis was rescued efficiently by constructs expressing LexA fused to the last 66 or 38 amino acids of Rip1p (LexA–RIP1-C66 and LexA–RIP1-C38, lanes 8 and 9) or to the last 43 residues of hCG1 (LexA–hCG1-C43, lane 10). These results show that the

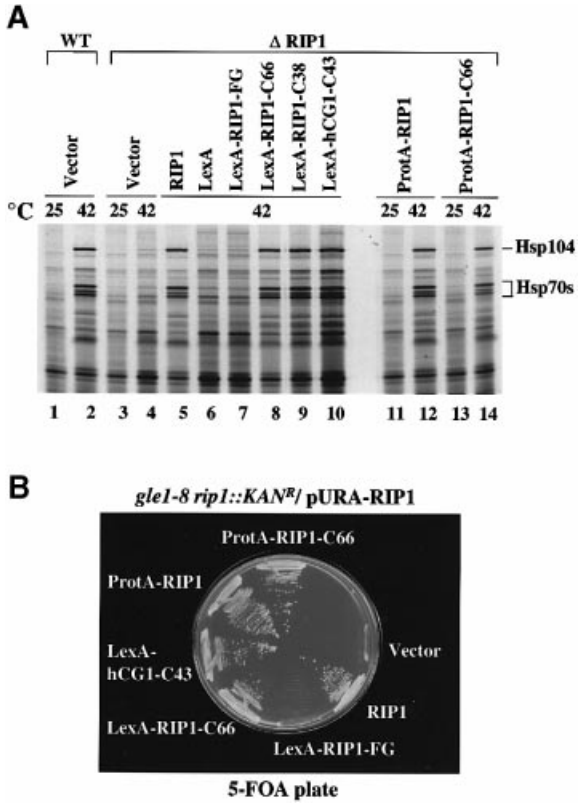

Fig. 2. hCG1 and Rip1p C-terminal domains are functionally homologous. (**A**) hCG1 and Rip1p C-termini rescue heat shock RNA export at 42°C in a *ΔRIP1* strain. Heat shock RNA export was assessed by examining heat shock protein synthesis at 25 or 42°C. The *ΔRIP1* strain was transformed with a LEU2/CEN vector (lanes 3 and 4) or plasmids expressing full-length Rip1p (RIP1, pFS398), LexA (pEG202), LexA–Rip1p-FG (pFS476), LexA–Rip1p-C66 (pFS1031), LexA–Rip1p-C38 (pFS1033), LexA–hCG1-C43 (pFS1035), ProtA–Rip1p (pFS829) or ProtA–Rip1p-C66 (pFS923) (lanes 5–14). The W303 wild-type strain, transformed with vector (LEU2/CEN), was analysed in parallel (lanes 1 and 2). Cultures of transformed strains were pre-heated for 15 min and subsequently labelled with [^{35}S]methionine for 15 min at the indicated temperatures. Total protein extracts were fractionated by SDS–PAGE and autoradiographed. (**B**) hCG1 and Rip1p C-termini rescue the synthetic lethality between the *gle1-8* mutant and a *RIP1* disruption. The *gle1-8* synthetic lethal strain covered by a RIP1 plasmid (*gle1-8*, *rip1::KAN^R*/pFS652 URA/CEN) was transformed with the plasmids described in (A). Rescue of synthetic lethality was assessed by streaking the transformants on medium containing 5-FOA.

last 38 amino acids of Rip1p, which are most highly conserved, are sufficient for function, and that the C-domains of hCG1 and Rip1p have the same functional properties. Finally, plasmids expressing protein A fused to full-length Rip1p or to the last 66 amino acids of Rip1p also efficiently rescued heat shock RNA export in the *ΔRIP1* strain (ProtA–RIP1 and ProtA–RIP1-C66; lanes 12 and 14). No heat shock protein synthesis was observed with LexA alone (LexA; lane 6) nor with LexA fused to the FG-repeat domain of Rip1p (LexA–RIP1-FG; lane 7).

Secondly, we tested whether the same constructs could rescue the *ΔRIP1* synthetic lethal phenotype of the *GLE1* mutant strain FSY38 (Figure 2B). This strain (*gle1-8*, *rip1::KAN^R*, pURA-RIP1) was isolated earlier in a *ΔRIP1* synthetic lethal screen (see below); it contains the *gle1-8* allele on the chromosome, a *RIP1* deletion and a wild-type *RIP1* plasmid (pFS652; URA3, CEN) to cover the synthetic lethality. The LexA–hCG1-C43 and LexA–RIP1-C66 constructs complemented synthetic lethality and allowed strain FSY38 to grow on 5-fluoro-orotic acid (5-FOA) as efficiently as the wild-type *RIP1* plasmid (pFS398). The LexA–RIP1-C38 construct also rescued the *gle1-8* synthetic lethality, albeit less efficiently (data not shown), and no growth was detected on 5-FOA in the presence of LexA–RIP1-FG or an empty vector. Finally, the ProtA–RIP1 and ProtA–RIP1-C66 constructs similarly rescued the *gle1-8* synthetic lethal mutation, showing that these fusions also function under normal growth conditions (Figure 2B and see below).

These data taken together demonstrate that the 43 C-terminal amino acids of hCG1 can substitute for the corresponding region of Rip1p under stress or normal growth conditions and support that hCG1 and Rip1p/Nup42p represent functional homologues.

Identification of extragenic high copy suppressors of a GLE1 temperature-sensitive mutant

The genetic interactions between Rip1p and Gle1p and the clear involvement of these two proteins in RNA export prompted us to explore further the genetic space around Gle1p. The *gle1-8* temperature-sensitive (ts) allele, identified as one of several *GLE1* alleles in an earlier *ΔRIP1* synthetic lethal screen (Stutz *et al.*, 1997), was used to screen for high copy extragenic suppressors. Gle1p comprises a non-essential N-terminal region (amino acids 1–112), an essential predicted coiled-coil domain (amino acids 113–255) and an essential C-terminal domain (amino acids 256–538), which contains the proposed Rev-like NES (Del Priore *et al.*, 1997; Watkins *et al.*, 1998; and Figure 3A). The *gle1-8* allele contains a T21A substitution in the N-terminal domain and an E340K change (upstream of the proposed NES) in the C-terminal domain likely to be responsible for the ts phenotype. Interestingly, all the *GLE1* alleles isolated in the *ΔRIP1* synthetic lethal screen contained mutations within the essential C-terminal domain, indicating a role for this region in the functional interaction with Rip1p.

High copy suppressors of the *gle1-8* mutant strain were identified by transformation of a yeast genomic library cloned into a 2μ-based high copy vector and selection of transformants at 37°C. Besides *GLE1*, the genes found most frequently and exhibiting the strongest suppression phenotype were *RIP1*, *RAT8/DBP5*, which encodes a DEAD-box protein essential for RNA export, and the uncharacterized open reading frame (ORF) *YMR255w*. This ORF has also been identified in a screen for high copy suppressors of a *RAT8/DBP5* mutant allele and was named *GFD1* (Hodge *et al.*, 1999). High level expression of Rip1p, Rat8p/Dbp5p or Gfd1p was not able to bypass a *GLE1* null allele (data not shown).

To determine how well these three genes in high copy suppressed the growth defect of *gle1-8* cells, the growth at 37°C of the *gle1-8* transformants was examined in liquid cultures or on plates (Figure 3B). Overexpression of Rip1p, Rat8p/Dbp5p and Gfd1p substantially, but not completely, rescued the *gle1-8* ts, since the strains transformed with high copy *RIP1*, *RAT8/DBP5* and *GFD1* plasmids did not grow as fast as that transformed with wild-type *GLE1*. The rescue appeared more potent on plates.

As the C-domain of Rip1p was able to complement the

synthetic lethality of a *ΔRIP1-gle1-8* strain (Figure 2B), we tested whether this domain would also exhibit high copy suppression of the *gle1-8* ts phenotype. The C-terminal 66 amino acids of Rip1p were expressed as a Gal-inducible GST fusion from a 2μ plasmid. The *gle1-8* growth defect was rescued substantially at 37°C upon expression of GST–Rip1p-C66 both in liquid and on plates. This phenotype was dependent on galactose (Figure 3C).

Mutations in Gle1p induce poly(A)$^+$ RNA export defects. We next examined the ability of the high copy suppressors to restore poly(A)$^+$ RNA export in the *rss1-37 (gle1)* ts strain (Saavedra *et al*., 1997; and see below) by *in situ* hybridization with an oligo(dT) probe (Figure 3D). The *rss1-37* strain (FSY292) transformed with an empty vector exhibited a strong nuclear poly(A)$^+$ RNA signal and very weak cytoplasmic staining after a 30 min incubation at 37°C (panel a). The RNA export defect was eliminated in the presence of a wild-type *GLE1* plasmid (panel b). High copy plasmids expressing Rip1p and Rat8p/Dbp5p significantly rescued poly(A)$^+$ RNA export, as all the cells exhibited substantial cytoplasmic staining and less frequent or weaker nuclear signal (panels c and d). Overexpression of Gfd1p had a detectable, but more modest effect (panel e). The incomplete restoration of poly(A)$^+$ RNA export in the *rss1-37* mutant at 37°C by overexpression of Rip1p, Rat8p/Dbp5p or Gfd1p parallels the partial suppression of the *gle1-8* and *rss1-37* growth phenotypes (Figure 3B and data not shown).

To determine whether the localization of gle1-8p was altered in the presence of the high copy suppressors, we chromosomally tagged the mutant gene with green fluorescent protein (GFP). The distribution of the gle1-8p–GFP fusion was examined in living cells at 25°C or after a shift to the non-permissive temperature in the presence of an empty vector or 2μ plasmids expressing Rip1p or Rat8p/Dbp5p (Figure 3E). The distribution of gle1-8p–GFP was compared with that of Gle1p–GFP in a chromosomally tagged wild-type strain. Like wild-type Gle1p–GFP, gle1-8p–GFP exhibited a typical nuclear rim staining. After a 4 h shift to the non-permissive temperature in the presence of an empty vector, the gle1-8p–GFP signal became modestly weaker than at 25°C or than in wild-type Gle1p–GFP cells grown at 37°C. Overexpression of Rip1p or Rat8p/Dbp5p marginally increased the fraction of gle1-8p–GFP present at the nuclear envelope at 37°C (Figure 3E). Western blot analysis showed that the steady-state levels of gle1-8p–GFP at 25°C were identical to those of wild-type Gle1p–GFP (Figure 3F, compare lanes 1 and 6); the gle1-8p–GFP levels remained stable over a 6 h incubation of the cells at 37°C and were not affected by overexpression of Rip1p, Rat8p/Dbp5p or Gfd1p (compare lanes 1–5). These data indicate that the high copy suppressors do not act by stabilizing the mutant protein. As the localization of gle1-8p–GFP was only modestly affected by overexpression of Rip1p or Rat8p/Dbp5p, it is not clear whether the high copy suppressors enhance the association of gle1-8p–GFP with the NPC, or whether they suppress the ts phenotype through a different process.

Physical interactions between Gle1p and the high copy suppressor proteins

To investigate the relationship between Gle1p and its high copy suppressors, we tested the physical interaction between these proteins in the two-hybrid assay (Table I). As full-length Gle1p two-hybrid fusions were poorly expressed, constructs were used that expressed the C-terminal domain of Gle1p (amino acids 257–538), which contains the proposed Rev-like NES (Figure 3A).

Consistent with the genetic observations, Gle1p bait strongly interacted with preys containing full-length or the C-terminal 66 or 38 residues of Rip1p but not with preys containing the FG-repeat domain of Rip1p. An identical pattern of interaction was observed with hCG1, verifying the functional homology between Rip1p and hCG1. The reciprocal Rip1p/hCG1p bait and Gle1p prey constructs gave the same results (Table I and data not shown). The interactions between Gle1p and the C-domains of Rip1p and hCG1 were weakened by the *gle1-8* mutation (E340K) and were completely abolished in the presence of the *rss1-37 (gle1)* ts allele. This latter *GLE1* mutant, obtained by PCR mutagenesis (Saavedra *et al*., 1997), exhibits a stronger growth defect than *gle1-8* and contains several mutations in the C-terminal domain. Western blot analysis confirmed equal expression of wild-type and mutant Gle1p two-hybrid fusions (data not shown).

As Gle1p was proposed to share functional characteristics with HIV-1 Rev, the two proteins were compared in these two-hybrid analyses. In contrast to Gle1p and consistent with our earlier data, the HIV-1 Rev bait fusion interacted with the FG-repeats of both Rip1p and hCG1 (presumably through bridging by Crm1p) but not with their C-termini (Table I). Taken together with the absence of an interaction between Gle1p and Crm1p, the data indicate that Gle1p does not behave like a bona fide NES-containing protein in this assay.

Lastly, we tested the two-hybrid interaction between Gle1p and prey fusions expressing full-length Rat8p/Dbp5p or Gfd1p prey fusions. The C-terminal domain of Gle1p strongly interacted with these two high copy suppressors, and both interactions were abolished by the *gle1-8* and *rss1-37* mutations. These results show that the three high-copy suppressors of the *gle1-8* mutant physically interact with the C-terminal region of Gle1p. In addition, we detected an interaction between Gfd1p and the FG-repeat domain of Rip1p (Table I) and between Rat8p/Dbp5p and Gfd1p (data not shown).

Gle1p interacts with its high copy suppressors in vitro

To test whether the two-hybrid interactions between Gle1p and the three suppressors may represent direct associations, the same proteins were tested for binding *in vitro*. Full-length Gle1p or its C-terminal domain were prepared by *in vitro* translation in reticulocyte lysates in the presence of [^{35}S]methionine. The ^{35}S-labelled Gle1 proteins were incubated with GST fusions produced in *Escherichia coli* and purified on glutathione beads (Figure 4). Full-length Gle1p specifically interacted with the C-terminal domains of Rip1p and hCG1 (GST–Rip1-C66 and GST–hCG1-C43), as well as with full-length Gfd1p and Rat8p/Dbp5p (GST–Gfd1 and GST–Rat8/Dbp5) (top panel, lanes 4–7). Gle1p did not interact significantly with the FG-repeat domain of Rip1p as the binding was not greater than with GST alone (top panel, compare lanes 2 and 3). Consistent with the two-hybrid data, the same pattern was obtained

in the presence of the truncated Gle1p protein with no substantial loss in binding efficiency, suggesting that the C-terminal region of Gle1p is responsible for these interactions (top two panels, compare Gle1p input with the amount of Gle1p bound to each GST fusion). None of the GST fusions interacted with *in vitro* translated luciferase (third panel), and Coomassie Blue staining of the polyacrylamide gels before autoradiography showed comparable GST fusion input in each binding reaction (lower panel). These data strongly indicate that Gle1p interacts directly with the three high copy suppressors; however, the possibility that some of these associations are mediated by components in the reticulocyte lysate cannot be discarded.

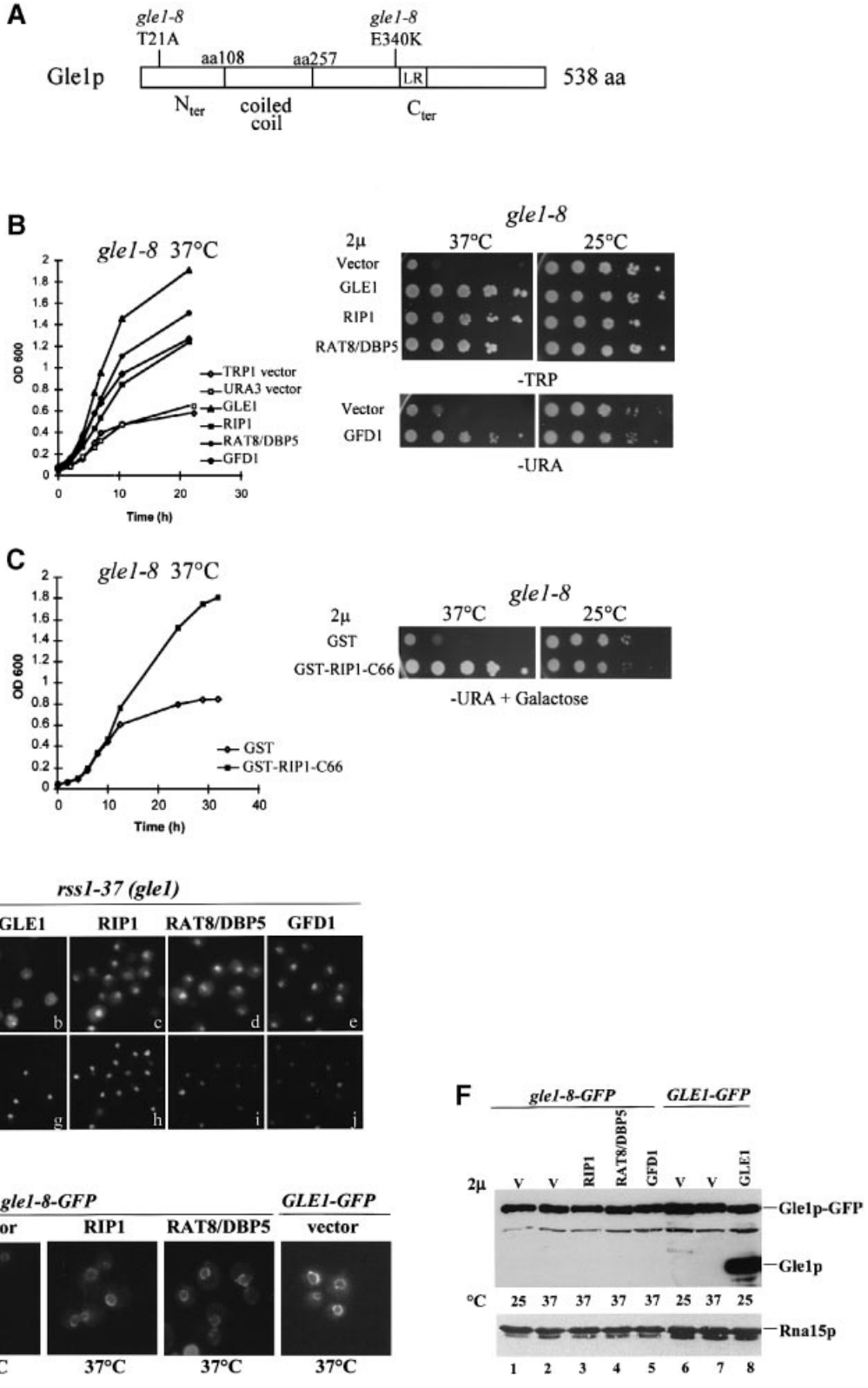

Poly(A)$^+$ RNA export is dependent on Rip1p in a GLE1 mutant background

The genetic and physical relationships between Gle1p and Rip1p strongly support the participation of Rip1p in RNA export through an interaction with Gle1p. To demonstrate further the importance of Rip1p in RNA export, we compared poly(A)$^+$ RNA distribution in two *ΔRIP1* synthetic lethal strains, FSY58 and FSY57, which contain the weak ts *gle1-1* allele (F381S substitution) and a *RIP1* disruption covered by a RIP1 plasmid. In FSY58, the RIP1 plasmid (pFS398) expresses normal levels of Rip1p (Rip1p normal); in FSY57, the RIP1 plasmid (pFS724) contains a truncated *RIP1* promoter which results in the production of 5–10 times less Rip1p (Rip1p low) (Stutz *et al*., 1997). Poly(A)$^+$ RNA distribution was examined in FSY58 and FSY57 by *in situ* hybridization with a digoxigenin-labelled oligo(dT) probe at 25°C or after a 30 min shift to 37°C (Figure 5). Both strains exhibited an enhanced nuclear accumulation of poly(A)$^+$ RNA at 37°C. However, the fraction of cells presenting an export defect was significantly higher in the strain expressing low levels of Rip1p both at 25°C (Figure 5, compare panels a and e) and 37°C (compare panels c and g). The enhanced poly(A)$^+$ RNA export defect exhibited by the *gle1-1* strain in the presence of limiting levels of Rip1p is consistent with a role for Rip1p in mRNA export.

Localization of Gle1p, Rip1p and Rat8p/Dbp5p by immunoelectron microscopy

Although Gle1p, Rip1p and Rat8p are clearly involved in RNA export, their exact contribution to this process is unknown. Defining the precise localization of these proteins within the NPC three-dimensional structure may help to assign them a role in specific steps of export. For this purpose, the location of Gle1p, Rip1p and Rat8p was determined at the ultrastructural level by performing pre-embedding labelling immunoelectron microscopy, a procedure which yields structurally intact yeast NPCs (Fahrenkrog *et al*., 1998). The proteins of interest were tagged with protein A and expressed in strains disrupted for the wild-type gene. The tagged proteins were detected with a colloidal gold-conjugated anti-protein A antibody. The ProtA–Gle1p and ProtA–Rat8p fusions are functional as they complement the corresponding lethal gene disruption (Murphy and Wente, 1996; Tseng *et al*., 1998). Two constructs that encoded protein A fused to full-length Rip1p (ProtA–Rip1p) or to the C-terminal 66 amino acids of Rip1p (ProtA–Rip1p-C66) were used to localize Rip1p.

Table I. Gle1p two-hybrid interactions

	Preys										
Baits	Rip1p	Rip1-FG	Rip1-C66	Rip1-C38	hCG1	hCG1-FG	hCG1-C43	Rat8p/ Dbp5p	Ymr255p/ Gfd1p	Gle1 (257–538)	Rev
Gle1 (257–538)	++	–	+++	+++	+++	+	+++	+++	+++	–	ND
gle1-8 (257–538)	++	–	++	–	+/–	–	+/–	–	–	–	ND
rss1-37 (257–538)	–	–	–	–	–	–	–	–	–	–	ND
Rip1-FG	–	–	–	–	–	–	–	–	++	–	+++
Rip1-C66	–	–	–	–	–	–	–	–	–	+++	–
Rev	+++	++	–	–	++	+++	–	–	–	–	+++
Crm1p	+	++	–	–	+++	+++	–	–	–	–	+++

The indicated bait and prey constructs were transformed into the RFY206 and EGY48 strain, respectively, and containing the β-galactosidase reporter construct pSH18-34. The transformants were mated on YEPD. Diploids were replica-plated on SD-Ura-His-Trp indicator plates containing 3% galactose/1% raffinose and X-gal. The strength of two-hybrid interactions was estimated visually by the intensity of the blue colour after 2 days at 30°C: +++ very dark blue; ++ blue; + light blue; – white; ND, not determined.

Fig. 3. Effects of the *GLE* high copy suppressors on growth, poly(A)$^+$ RNA distribution and localization of gle1-8p–GFP. (**A**) Gle1p contains a non-essential N-terminus followed by a coiled-coil region (amino acids 108–256) and a C-terminal domain with a putative leucine-rich (LR) NES. The amino acid changes present in the *gle1-8* allele are indicated. (**B**) The *GLE1* high copy suppressors partially rescue the growth defect of the *gle1-8* strain at 37°C. Strain *gle1-8* was transformed with control vectors (URA3 or TRP1, 2μ) or high copy plasmids (pFS998, pFS997, pFS999 or pFS952) expressing Gle1p, Rip1p, Rat8p/Dbp5p or Gfd1p, respectively. Liquid cultures of the transformed strains were diluted to OD_{600} = 0.03, grown for 2 h at 25°C and shifted to 37°C. Growth was followed by measuring optical density at 600 nm over time (left). The *gle1-8* transformants were also compared for growth on solid medium by spotting dilution series of saturated cultures on selective plates at 25 or 37°C (right). (**C**) The Rip1p C-terminus partially rescues the growth defect of the *gle1-8* strain at 37°C. Strain *gle1-8 was* transformed with the Gal-GST vector (pYGEX2T, URA/2μ) or the galactose-inducible GST–RIP1-C66 construct (pFS961) and growth was monitored at 37°C in SD-Ura medium containing galactose (left); growth was also examined on SD-Ura plates containing galactose at 25 or 37°C (right), as described above. (**D**) The *GLE1* high copy suppressors partially rescue the poly(A)$^+$ RNA export defect of the temperature-sensitive strain *rss1-37* (*gle1*) at 37°C. Strain *rss1-37* (FSY292) was transformed with empty vector or with high copy (2μ) plasmids expressing Gle1p, Rip1p, Rat8p/Dbp5p or Gfd1p. Transformants were grown to mid-log phase at 25°C and subjected to a 30 min incubation at 37°C before fixation and *in situ* hybridization with a digoxigenin-labelled oligo(dT) probe for localization of poly(A)$^+$ RNA. Panels a–e show the fluorescence after the cells were probed with FITC-conjugated anti-digoxigenin antibody. Panels f–j show DAPI staining of the same cells, respectively, and indicate the position of the nuclei. (**E**) The NPC localization of gle1-8p–GFP is modestly enhanced at 37°C by high level expression of Rip1p or Rat8p/Dbp5p. The chromosomally tagged *gle1-8-GFP* (FSY399) and *GLE1-GFP* (FSY398) strains were transformed with empty vector or high copy (2μ) plasmids expressing Rip1p or Rat8p/Dbp5p. Cells grown to mid-log phase were kept at 25°C or shifted to 37°C for 4 h and examined directly under the microscope. (**F**) The levels of gle1-8p–GFP are stable and not affected by the high copy suppressors. The chromosomally tagged *gle1-8-GFP* (FSY399) and *GLE1-GFP* (FSY398) strains were transformed with an empty vector (V; lanes 1, 2, 6 and 7) or high copy plasmids expressing Rip1p, Rat8p/Dbp5p, Gfd1p (lanes 3–5) or Gle1p (lane 8). The transformants were grown at 25°C or incubated for 6 h at 37°C as indicated. Protein extracts from equivalent number of cells were subjected to Western blot analysis with a rabbit polyclonal antibody against Gle1p. The positions of GFP-tagged and non-tagged Gle1p are indicated. The same blot was probed with an anti-Rna15p antibody as a control for loading.

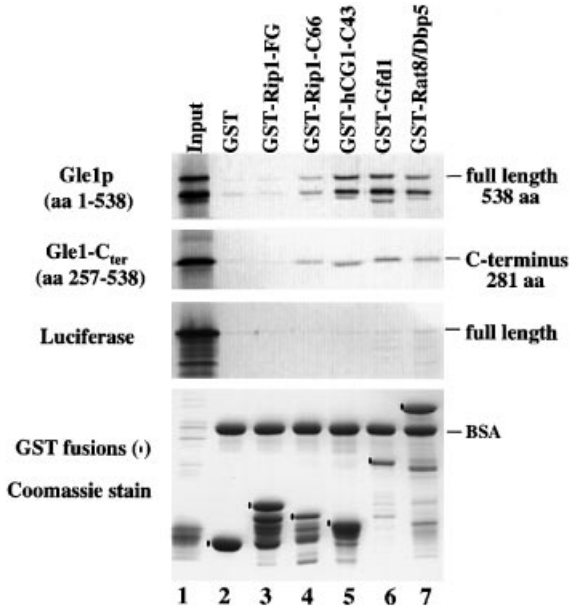

Fig. 4. Gle1p interacts with Rip1p, hCG1, Dbp5p/Rat8p and Gfd1p *in vitro*. GST alone or GST fusions containing the FG-repeat or C-terminal domains of Rip1p, the C-domain of hCG1, as well as full-length Gfd1p or Rat8p/Dbp5p were produced in *E.coli* and purified on glutathione beads. GST fusions on beads were tested for interaction with *in vitro* translated and [^{35}S]methionine-labelled full-length Gle1p, Gle1p C-terminal region (amino acids 257–538) or luciferase. After binding and washing, beads boiled in sample buffer were analysed by SDS–PAGE and bound ^{35}S-labelled proteins revealed by autoradiography (three top panels, lanes 2–7). Input (lane 1) corresponds to the amount of [^{35}S]protein added to each binding reaction. The amounts of GST fusions in each reaction were compared by Coomassie staining of a gel before autoradiography (lower panel; each GST fusion is indicated by a dot). BSA was used as non-specific competitor in the binding reactions and co-migrates on these gels.

These ProtA fusions are functional as well, since they efficiently rescued phenotypes associated with the *RIP1* deletion (Figure 2).

Gle1p is associated with NPC cytoplasmic fibrils. Consistent with earlier immunofluorescence studies (Del Priore *et al*., 1996; Murphy and Wente, 1996), Gle1p was detected in the cytoplasm but a significant fraction was found in association with NPCs. Interestingly, all the gold particles localized on the cytoplasmic side of the NPC, ~40–50 nm from the central plane, indicating an association with the cytoplasmic fibrils. Quantitative analysis of the labelling with respect to the centre of the 8-fold symmetry axis showed that Gle1p distributes over the whole diameter of the pore (Figure 6A and B). Given the physical interaction between Gle1p and Rip1p, we examined ProtA–Gle1p distribution in a *ΔGLE1/ΔRIP1* double deletion background (Figure 6C). Surprisingly, the ProtA–Gle1p staining was mostly lost from the NPCs, and gold particles were only found in the cytoplasm. Rip1p being inessential, it is unlikely to represent a major binding site for Gle1p at the NPC. One explanation for the drastic effect of the *RIP1* deletion on ProtA–Gle1p localization is that this fusion is not fully functional and is more sensitive to the absence of Rip1p; indeed, a strain expressing ProtA–Gle1p grows normally in the presence of Rip1p but is temperature sensitive when *RIP1* is deleted (data not shown). The data suggest that Rip1p contributes to the association of Gle1p with the NPC.

ProtA–Rat8p is cytoplasmic and associated with the cytoplasmic fibrils. Indirect immunofluorescence experiments have localized Rat8p/Dbp5p in the cytoplasm and in association with NPCs (Snay-Hodge *et al*., 1998; Tseng *et al*., 1998). By immunogold localization, the ProtA–Rat8p fusion was detected in the cytoplasm and on the cytoplasmic fibrils, with an apparent exclusion from the nuclear compartment (Figure 7A and B). These data are consistent with an association of Rat8p/Dbp5p with NPC

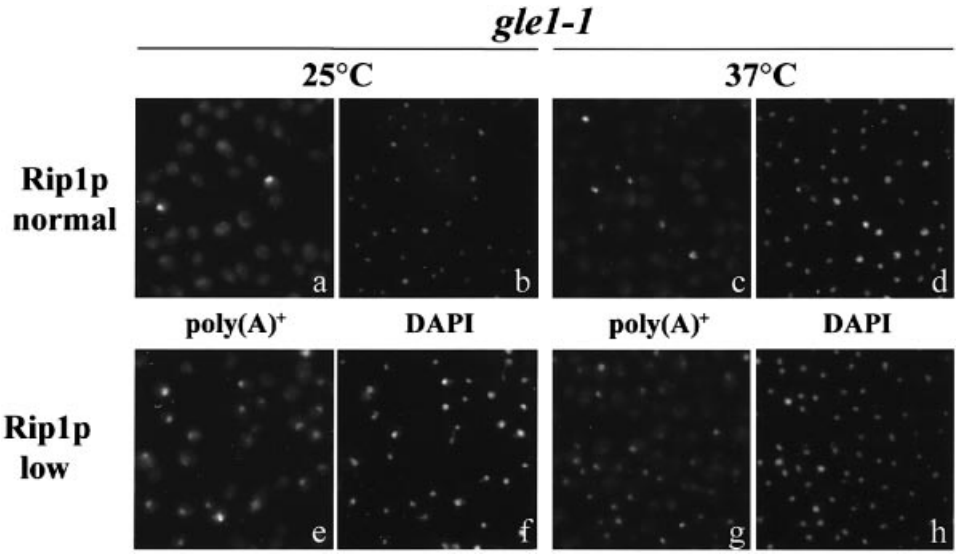

Fig. 5. Limiting levels of Rip1p enhance the poly(A)$^+$ RNA export defect of a *GLE1* mutant strain. Strains FSY58 (*gle1-1*, *rip1::KAN^R*/pFS398) and FSY57 (*gle1-1*, *rip1::KAN^R*/pFS724) expressing normal (wild-type) and low levels of Rip1p, respectively, were grown to mid-log phase at 25°C and either kept at 25°C or subjected to a 30 min incubation at 37°C. Cells were processed for *in situ* hybridization as described in Figure 3D. (**a**, **c**, **e** and **g**) The distribution of poly(A)$^+$ RNA; (**b**, **d**, **f** and **h**) DAPI staining of the same cells, respectively.

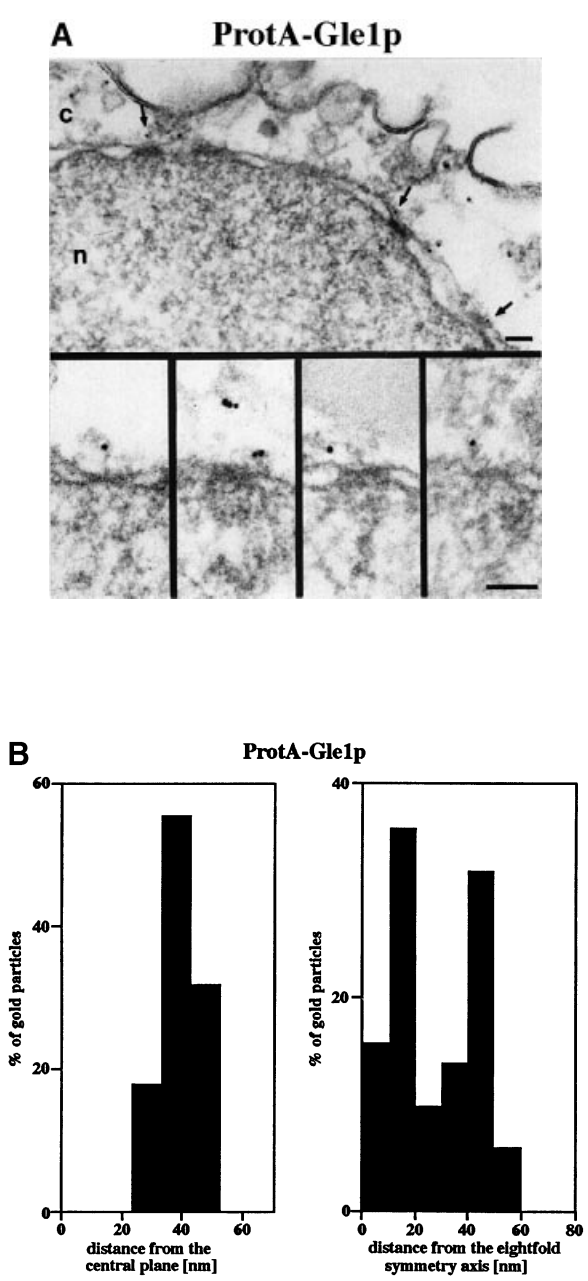

Fig. 6. Gle1p is located in the cytoplasm and on the cytoplasmic fibrils of the NPC. (**A**) Triton X-100-extracted spheroplasts from cells expressing ProtA–Gle1p in a *ΔGLE1* background (FSY251) were labelled with a polyclonal anti-protein A antibody conjugated to 8 nm colloidal gold and prepared for electron microscopy. Shown is a view along a cross-sectioned nuclear envelope (NE) stretch with labelled NPCs (arrows), together with a gallery of selected samples of labelled NPCs. The antibody labelled the cytoplasm and the cytoplasmic fibrils of the NPC. (**C**) In a *ΔGLE1ΔRIP1* background (FSY252), ProtA–Gle1p was located only in the cytoplasm of Triton X-100-extracted spheroplasts, but not at the NPC. Shown are two stretches along the NE on cross-sections. c, cytoplasm; n, nucleus. (**B**) Quantitative analysis of the gold particles associated with the NPCs in the ProtA–Gle1p *ΔGLE1* strain after labelling with gold-conjugated anti-protein A antibody. Fifty gold particles were scored. Bars, 100 nm.

proteins present on the cytoplasmic side of the pore and suggest that Rat8p/Dbp5p acts at a late step of RNA export.

Rip1p is found at two distinct sites of the NPC. The distribution of Rip1p contrasted with that of Gle1p. ProtA–Rip1p was detected in the nucleoplasm and on both sides of the NPC, in association with the nuclear baskets as well as with the cytoplasmic fibrils (Figure 8A). The quantification of the staining indicated the presence of similar amounts of Rip1p on both sides of the NPC; the distribution of Rip1p on the cytoplasmic fibrils was comparable with that of Gle1p, with a slightly higher concentration at the centre of the pore (Figure 8B). The detection of both Rip1p and Gle1p on the cytoplasmic fibrils, their physical interaction together with the enhanced RNA export defect in a *GLE1* mutant when Rip1p is limiting support that Rip1p contributes to a late step of RNA export through an interaction with Gle1p on the cytoplasmic fibrils. The overall distribution of Rip1p was unchanged in a *gle1-8* mutant background, suggesting that the localization of Rip1p is not dependent on a strong interaction with Gle1p (data not shown).

To examine the role of the FG-repeat versus the C-terminal domain of Rip1p in this distribution, we next localized a ProtA fusion containing only the unique C-terminus of Rip1p (ProtA–Rip1p-C66). Like full-length ProtA–Rip1p, ProtA–Rip1p-C66 was found within the nucleoplasm and on both sides of the NPC, indicating that the unique C-domain is sufficient to accumulate the fusion within the nucleus and to anchor Rip1p on both sides of the pore. In contrast to full-length Rip1p, the ProtA–Rip1p-C66 fusion was detected at a higher frequency on the cytoplasmic fibrils than on the nuclear baskets (Figure 8C and D). These observations could suggest that the FG-repeat domain of Rip1p stimulates

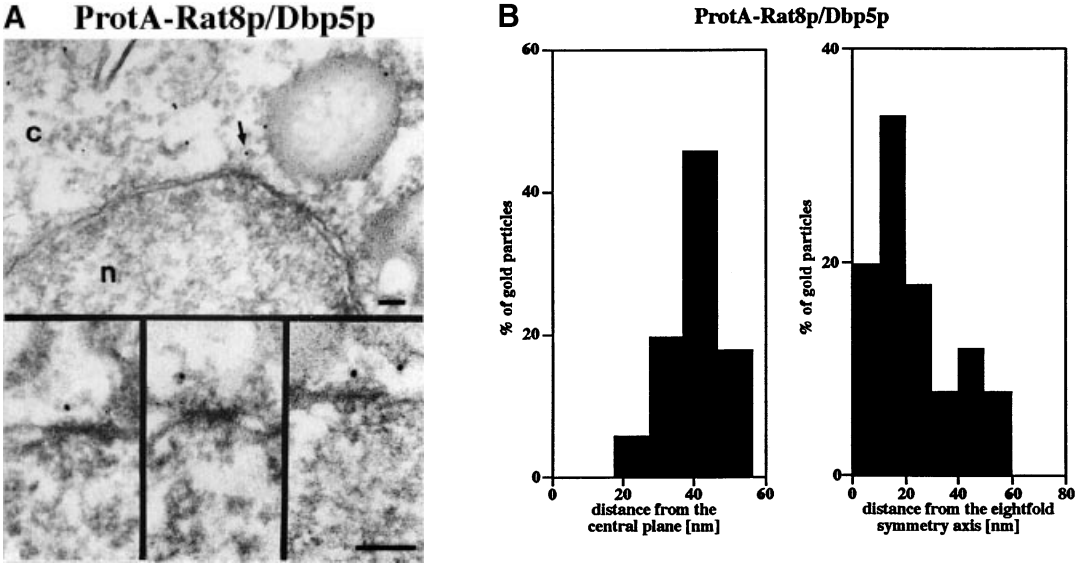

Fig. 7. Rat8p/Dbp5p is located in the cytoplasm and on the cytoplasmic fibrils of the NPC. (**A**) Triton X-100-extracted spheroplasts from cells expressing ProtA–Rat8p/Dbp5p in a *ΔRAT8/DBP5* background (FSY342) were prepared as described in Figure 6. Shown is a view of a cross-sectioned NE stretch with labelled NPCs (arrows) and a gallery of selected gold-labelled NPCs. c, cytoplasm; n, nucleus. (**B**) Distribution of the gold particles associated with the NPCs. Fifty gold particles were scored. Bars, 100 nm.

the recruitment of Rip1p to the nuclear baskets. Alternatively, if Rip1p was trafficking between the two sides of the pore, the FG-repeats could increase the recycling of Rip1p from the cytoplasmic to the nuclear side of the NPC. Finally, given the essential role of Rip1p under heat shock conditions, we examined the localization of ProtA–Rip1p in a *ΔRIP1* background after a 10 min shift to 42°C. The overall distribution of Rip1p at the NPCs was not substantially affected under these stress conditions (data not shown).

Since through pre-embedding labelling, some cytoplasmic epitopes can be lost (the cells are treated with Triton X-100 to facilitate labelling on both sides of the NPC), we cannot exclude that a small fraction of Rip1p is also present in the cytoplasm.

In vivo localization of Gle1p–GFP and Rat8p/Dbp5p–GFP in mutant backgrounds

Immunoelectron microscopy localization of ProtA–Gle1p showed that Gle1p was lost from the NPC in an *RIP1* deletion strain, suggesting a contribution of Rip1p to the association of Gle1p with the NPC (Figure 6C). To substantiate this observation, we examined the distribution of a Gle1p–GFP fusion in living cells in a *ΔGLE1* strain or a *ΔGLE1ΔRIP1* double deletion strain (Figure 9A). Similarly to the ProtA–Gle1p fusion, the Gle1p–GPF fusion conferred a ts phenotype in the absence of Rip1p, indicating that Gle1p–GFP was not fully functional (data not shown). Consistent with the immunoelectron microscopy data, the amount of Gle1p–GFP detected in association with the nuclear envelope after growing the cells at 37°C for 4 h was considerably lower in the absence of Rip1p. The disappearance of Gle1p–GFP from the NPC did not result from increased turnover or decreased synthesis, since the steady-state levels of Gle1p–GFP in the *ΔRIP1* strain were stable at 37°C over at least 6 h (data not shown). The localization of Gle1p appeared to be affected more drastically by the absence of Rip1p when examined by immunoelectron microscopy. This difference may be due to the fact that the electron microscopy data are from the quantitation of gold particles in cell sections, while the intensity of GFP fluorescence is derived from whole cells.

An *in vivo* interaction between Gle1p and Rat8p/Dbp5p was suggested by the high copy suppression and protein interaction assays. To determine whether Gle1p contributes to the association of Rat8p/Dbp5p with the NPC, a Rat8p/Dbp5p–GFP fusion was localized in a strain containing the *rss1-37 (gle1)* mutant allele (Figure 9B). The *rss1-37* mutation induces a strong poly(A)$^+$ RNA export defect and abolishes the two-hybrid interaction between Gle1p and Rat8p/Dbp5p (Figure 3D and Table I). Two strains were examined, both of which contained the *rss1-37* allele and expressed a Rat8p/Dbp5p–GFP fusion. In one case, the *RAT8/DBP5* gene was tagged with GFP on the chromosome (*rss1-37 RAT8/DBP5-GFP*); in the other, genomic *RAT8/DBP5* was deleted and Rat8p/Dbp5p–GFP expressed from a plasmid (*rss1-37 ΔRAT8/DBP5* pRAT8/DBP5-GFP; Figure 9B, right). Both strains behaved similarly. At 25°C, Rat8p/Dbp5p–GFP was detected in the cytoplasm as well as in association with the NPC, resulting in a strong nuclear rim staining as described (Snay-Hodge *et al*., 1998). After 2 h at 37°C, the GFP staining at the rim became weaker and more diffuse but did not disappear (even after prolonged exposure to 37°C); there was a concomitant modest increase in the cytoplasmic signal. These data are consistent with the notion that Gle1p represents a binding site for Rat8p/Dbp5p at the nuclear pore, but that other interactions are involved in the recruitment of this DEAD-box protein to the NPC.

Discussion

In this study, we used a high copy suppressor approach to identify proteins functionally or physically related to Gle1p. The screen identified the NPC-associated nucleoporin Rip1p, the DEAD-box protein Rat8p/Dbp5p and a new non-essential protein Ymr255p. This protein was

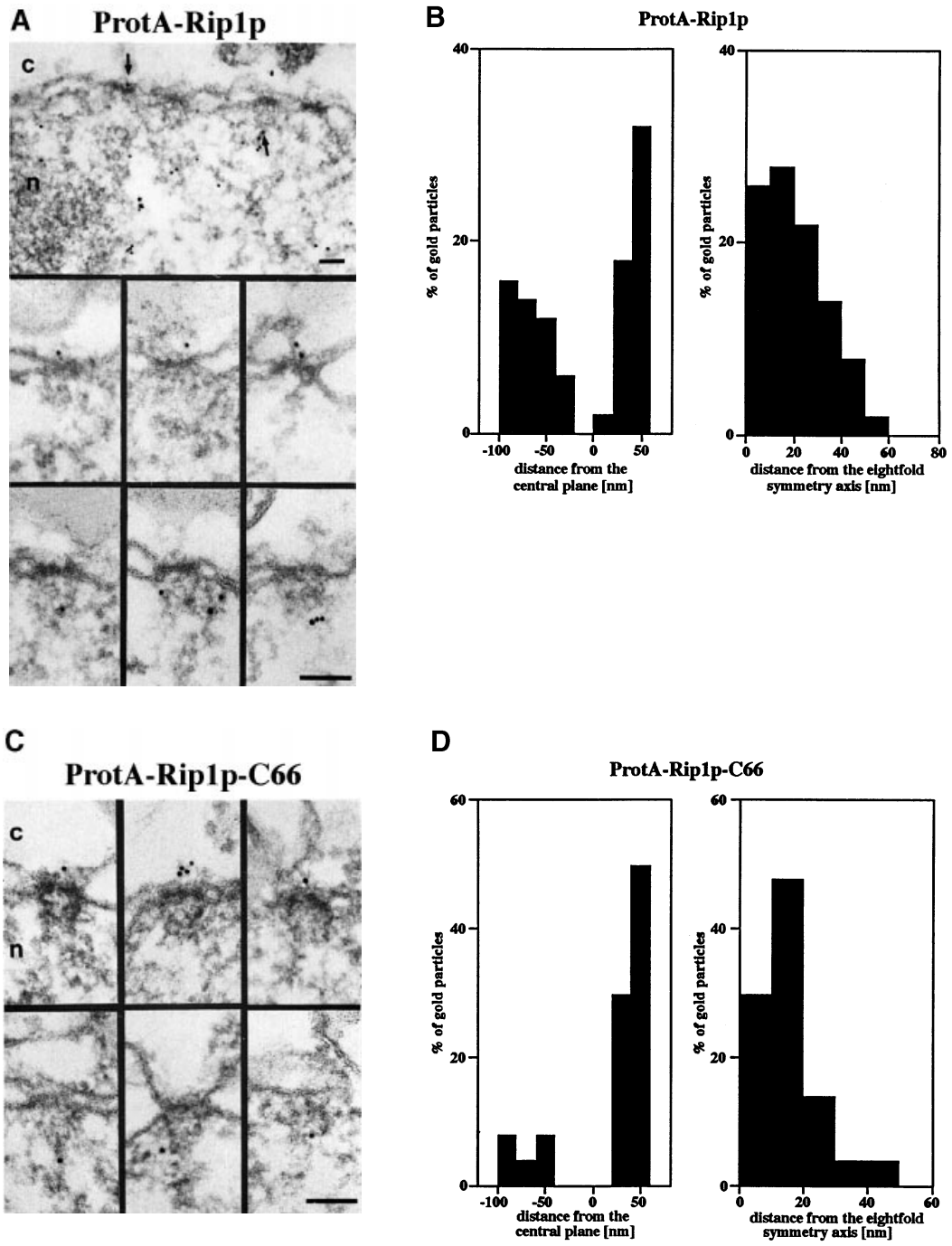

Fig. 8. Rip1p resides in the nucleus and on both the cytoplasmic and the nuclear face of the NPC. (**A**) Cells expressing ProtA–Rip1p in a *ΔRIP1* background (FSY221) were prepared as described in Figure 6. The anti-protein A antibody conjugated to 8 nm colloidal gold was found in the nucleus (overview, top), and in association with the cytoplasmic fibrils (middle) and the nuclear basket (bottom) of the NPC. This location of Rip1p remained the same in the ProtA–Rip1p-C66 *ΔRIP1* strain (FSY 329) (**C**). Arrows point to labelled NPCs in the overviews. c, cytoplasm; n, nucleus. The quantitative analysis of the gold particles associated with the NPCs (**B** and **D**) revealed an equal distribution on both sides of the NPC in the ProtA–Rip1p *ΔRIP1* cells, whereas in the ProtA–Rip1p-C66 *ΔRIP1* cells the cytoplasmic epitope was labelled significantly more frequently than the nuclear epitope of the NPC. Fifty gold particles were scored. Bars, 100 nm.

identified independently as a high copy suppressor of *RAT8/DBP5* (Hodge *et al*., 1999) and named Gfd1p. Our two-hybrid and *in vitro* binding assays indicate that the essential C-terminal domain of Gle1p interacts directly with Rip1p, Rat8p/Dbp5p and Gfd1p (Table I and Figure 4). These data together with the synthetic lethal interactions between Gle1p, Rip1p and Rat8p/Dbp5p (Stutz *et al*., 1997; Snay-Hodge *et al*., 1998) are consistent with a functional association of these proteins *in vivo.*

Gle1p initially was proposed to contain a Rev-like NES in its essential C-terminal domain and to promote poly(A)$^+$ RNA export through an NES-dependent export pathway involving an interaction with Rip1p, analogous to that described between Rev-NES and the FG-repeat domain of Rip1p (Murphy and Wente, 1996). However, the NES is not conserved in the human homologue of Gle1p (Watkins *et al*., 1998), and the localization of Gle1p–GFP at the nuclear rim was not affected in the *xpo1-1* (*crm1*)

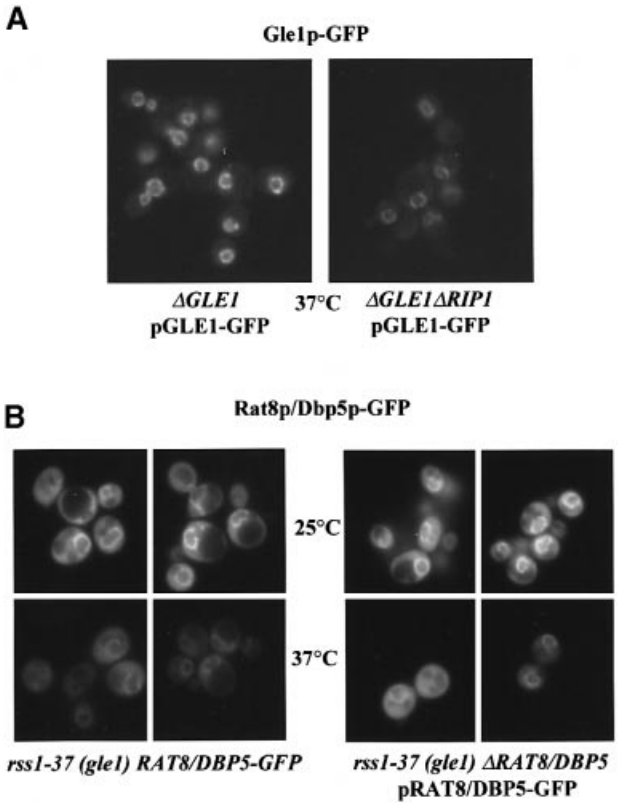

Fig. 9. (**A**) The localization of Gle1p–GFP at the NPC is weakened in the absence of Rip1p. *ΔGLE1* (FSY297) or *ΔGLE1-ΔRIP1* (FSY298) strains expressing Gle1p–GFP from a centromeric plasmid (pFS1030) were grown at 25°C in selective medium to mid-log phase, shifted to 37°C for 4 h and examined under the microscope. (**B**) Rat8p/Dbp5p–GFP is partially lost from the NPC in the *rss1-37 (gle1)* mutant background. Rat8p/Dbp5p–GFP was localized in two strains containing the *rss1-37* allele. The strain on the left (*rss1-37 RAT8/DBP5-GFP*; FSY400) contains a *RAT8/DBP5* gene chromosomally tagged with GFP. The strain on the right (*rss1-37 ΔRAT8/DBP5* pRAT8/DBP5-GFP; FSY401) contains a *RAT8/DBP5* deletion covered by a plasmid (pCS835) expressing a Rat8p/Dbp5p–GFP fusion. The strains were grown in SD complete medium to mid-log phase at 25°C. They were then kept at 25°C or shifted to 37°C for 2 h and examined under the microscope. Two fields are shown for each strain at 25 and 37°C.

ts strain (Stade *et al*., 1997). The physical interaction between Gle1p and Rip1p further shows that Gle1p does not behave like a Rev-NES-containing protein. Indeed, the Gle1p essential C-domain interacts directly with the unique C-domain of Rip1p rather than its FG-repeat region (Table I and Figure 4); the association between these two proteins is therefore clearly distinct from that between Rev-NES and the Rip1p FG-repeats, which is bridged by the NES export factor Crm1p (Neville *et al*., 1997); consistently, neither we nor others were able to detect an interaction between Gle1p and Crm1p (Watkins *et al*., 1998) (Table I).

Although rapid movement of Gle1p in and out of the nucleus cannot be excluded, the immunoelectron microscopic detection of Gle1p uniquely in the cytoplasm and on the cytoplasmic fibrils further supports that Gle1p is not a shuttling protein; however its association with the pore may be dynamic (Figure 6). Like Gle1p, Rat8p/Dbp5p was localized in the cytoplasm and in association with the cytoplasmic fibrils by immunoelectron microscopy (Figure 7; Schmitt *et al*., 1999). Gfd1p was located in the cytoplasm and at the nuclear rim by indirect immunofluorescence, a distribution similar to that of Rat8p/Dbp5p (Hodge *et al*., 1999). A substantial fraction of Rip1p was also found in association with the cytoplasmic fibrils (Figure 8). These distributions, together with the genetic and physical interaction data, are consistent with the view that Gle1p, Rip1p, Rat8p/Dbp5p and Gfd1p functionally interact on the cytoplasmic face of the NPC and participate in one or more late steps of RNA export.

These observations raise the question of whether Gle1p interacts with its high copy suppressors simultaneously to form a single complex or whether some of these interactions are mutually exclusive. In this latter case, Gle1p may combine with its partners to form different sub-complexes with redundant or complementary functions. Alternatively, the C-terminal domain of Gle1p may undergo sequential interactions with Rip1p, Rat8p/Dbp5p and Gfd1p, which may be part of a series of events contributing to the release of an RNP from the NPC.

Based on the localization and interaction data, the synthetic lethality between a *RIP1* deletion and *GLE1* mutations is probably due to the absence of the *RIP1* C-terminal domain from the cytoplasmic fibrils. This is because synthetic lethality is rescued by the Rip1p C-terminus alone, and overexpression of this domain is able to suppress a temperature-sensitive *GLE1* mutation (Figures 2 and 3). A contribution of Rip1p to Gle1p function is also supported by the enhanced RNA export defect in a *GLE1* mutant strain when Rip1p becomes limiting (Figure 5). One interpretation of these observations is that the binding of the C-domain of Rip1p to Gle1p stimulates Gle1p activity, perhaps by optimizing the association of Gle1p with some of its partners (e.g. Rat8p/Dbp5p or Gfd1p). This function of Rip1p becomes essential in a *GLE1* mutant background or under stress conditions, where the overall efficiency of RNA export is reduced.

Two biochemically defined NPC sub-complexes with primary roles in poly(A)$^+$ RNA export have been described. One is composed of the essential nucleoporins Nup159p/Nup82p/Nsp1p (Belgareh *et al*., 1998; Hurwitz *et al*., 1998) and the other consists of Nup84p/Nup85p/Nup120p/C–Nup145/Seh1p/Sec13p (Siniossoglou *et al*., 1996; Teixeira *et al*., 1997). Members of both sub-complexes have been localized on the NPC cytoplasmic fibrils (Kraemer *et al*., 1995; Fahrenkrog *et al*., 1998; Hurwitz *et al*., 1998; Katahira *et al*., 1999; Stoffler *et al*., 1999). It is noteworthy that these distributions may not all be evolutionarily conserved, as components of a human NPC sub-complex, homologous to the Nup84p sub-complex, have been located at the nuclear basket (Fontoura *et al*., 1999). The exact function of these complexes in pore structure versus export function is still poorly defined. More specific roles have been attributed to individual components. Nup82p, for example, anchors the corresponding complex within the NPC (Belgareh *et al*., 1998), whereas Nup159p or components of the Nup84p complex provide binding sites for shuttling proteins involved in more dynamic aspects of export (Santos-Rosa *et al*., 1998; Schmitt *et al*., 1999; and see below).

No physical connections have yet been established between the Nup84p and Nup159p sub-complexes, but

multiple genetic interactions functionally relate these two sets of proteins (reviewed in Fabre and Hurt, 1997). Similarly, multiple genetic interactions link Gle1p and its partners to the two defined sub-complexes (Del Priore *et al*., 1996; Stutz *et al*., 1997; Hurwitz *et al*., 1998; Snay-Hodge *et al*., 1998), suggesting that a number of these NPC components have overlapping or redundant functions. Alternatively, these proteins may all belong to a single multifunctional complex participating in several sequential steps of RNA export.

The identification of the DEAD-box protein Rat8p/Dbp5p as a partner for Gle1p and the substantial decrease of Rat8p/Dbp5p–GFP rim staining in the *rss1-37* (*gle1*) temperature-sensitive mutant background suggest that Gle1p participates in the binding of Rat8p/Dbp5p to the nuclear pore (Figure 9B). However, the partial retention of Rat8p/Dbp5p–GFP at the NPC in the mutant background at 37°C is consistent with the existence of alternative binding sites. Indeed, a direct interaction between Rat8p/Dbp5p and the N-terminal domain of Rat7p/Nup159p has been identified (Hodge *et al*., 1999; Schmitt *et al*., 1999). These observations could explain the suppression of the *rat7-1*/*nup159-1* temperature-sensitive mutation by high level expression of Gle1p (Del Priore *et al*., 1996), i.e. an excess of Gle1p may provide additional binding sites for Rat8p/Dbp5p when the mutant rat7-1p/nup159-1p is degraded, and thereby partially restore poly(A)$^+$ RNA export.

The ProtA–Gle1p and Gle1p–GFP fusions are substantially lost from the NPC in the absence of Rip1p (Figures 6C and 9A); these strains are also temperature sensitive for growth indicating that Rip1p contributes to a functionally relevant association of Gle1p with the NPC. As Rip1p is inessential, it is unlikely to represent a major binding site for Gle1p. Consistently, such a role for Rip1p is revealed only in the presence of the ProtA–Gle1p and Gle1p–GFP fusions, which are not fully functional proteins (see Results). Rip1p may therefore strengthen the association of Gle1p with the nuclear pore, presumably by stabilizing Gle1p within a complex. The major anchoring site for Gle1p at the pore is not known, but it may involve the essential coiled-coil domain of Gle1p, by analogy to other NPC proteins (Belgareh *et al*., 1998).

The immunoelectron microscopic localizations detected Rip1p within the nucleoplasm and the NPC nuclear baskets and cytoplasmic fibrils, a distribution distinct from that observed for Gle1p and Rat8p/Dbp5p. The presence of Rip1p on both sides of the NPC suggests that this FG-nucleoporin may have a role in late as well as in early steps of export, i.e. the recruitment of export complexes from the nucleoplasm towards the baskets. Rip1p may then move from one side to the other, perhaps in association with cargoes, and participate in their release on the cytoplasmic side of the NPC. The accumulation of Rip1p at two distinct NPC sites may reflect rate-limiting steps during that process. The vertebrate NPC-associated FG-nucleoporins Nup98 and Nup153 recently have been proposed to move between the nuclear and cytoplasmic compartments in association with exported cargoes (Nakielny *et al*., 1999; Zolotukhin and Felber, 1999)

An association of Rip1p with RNP cargo was suggested by the identification of an interaction between the human RNA export factor TAP and the FG-nucleoporins CAN/Nup214 and hCG1, the functional homologues of Nup159p and Rip1p, respectively (Katahira *et al*., 1999; E.Izaurralde, personal communication; and Figure 2). These data support the view that TAP and its yeast homologue Mex67p promote the export of bound RNPs through an interaction with one or more FG-nucleoporins (de Castillia and Rout, 1999). Consistent with the TAP–hCG1 interaction, we observed a homologous two-hybrid interaction between Mex67p and the FG-repeat domain of Rip1p (D.Zenklusen, unpublished results).

The association of Mex67p with the NPC is essential for RNA export, and this interaction is mediated by Mtr2p. Nup85p, a component of the Nup84p sub-complex, represents one target of the Mex67p/Mtr2p complex at the NPC (Santos-Rosa *et al*., 1998). Interestingly, we identified several *NUP85* alleles in the *ΔRIP1* synthetic lethal screen that were only rescued by full-length Rip1p (our unpublished data). These genetic observations together with the Mex67p/Rip1p–FG two-hybrid interaction suggest that the FG-repeat domain of Rip1p may complement Nup85p by contributing to the association of Mex67p with the pore. As the immunoelectron microscopic distributions of Rip1p and Mex67p are comparable (Santos-Rosa *et al*., 1998; and Figure 8), Rip1p could associate with Mex67p within the nucleus and travel along with the RNP complex through the NPC. On the cytoplasmic side, Rip1p is likely to interact with Gle1p through its C-terminus; this interaction may in turn stimulate the association of Gle1p with the DEAD-box protein Rat8p/Dbp5p. ATP binding and hydrolysis may drive conformational rearrangements within associated RNPs, which ultimately will result in the release of the RNP from the NPC and/or the recycling of RNP components towards the nucleus. As the RNA-unwinding activity of Rat8p/Dbp5p *in vitro* is dependent on a co-factor (Tseng *et al*., 1998), Gle1p and/or its associated proteins could be candidates for such a function.

In summary, our data support the notion that Gle1p acts in a terminal step of RNA export through an interaction with multiple partners. Further studies will address the molecular details of these interactions and possibly reveal aspects of the dynamic rearrangements underlying export. The ability of hCG1 to rescue a *RIP1* deletion is consistent with the functional conservation of Rip1p during evolution. Our data support that hCG1 represents the true homologue of Rip1p, which is distinct from the earlier described hRIP/RAB1 protein (Bogerd *et al*., 1995; Fritz *et al*., 1995); the extent of conservation between all of the partners of hCG1 in yeast and in vertebrate systems will be investigated in the future.

Materials and methods

The DNA manipulations were performed according to standard methods. Yeast media and yeast transformations were performed with established procedures (Ausubel *et al*., 1994). The strains and plasmids used in this study are listed in Tables II and III.

Yeast plasmid constructions

ProtA–RIP1 (pFS829) was obtained by introducing a *Sal*I site after the ATG of *RIP1* in pFS398 to generate pFS800. A 400 bp *Sal*I PCR product containing two IgG-binding domains from protein A was introduced into the *Sal*I site of pFS800 to generate pFS829. ProtA–RIP1-C66 (pFS923) was generated by deleting the FG-repeat domain in pFS829; briefly, a 1.6 kb *Hin*dIII–*Xho*I PCR fragment extending from the 5′

Table II. Yeast strains used in this study

Name	Description	Genotype	Source
W303		**a**, *ade2, his3, leu2, trp1, ura3*	
FSY17	W303 ΔRIP1	**a**, *ade2, his3, leu2,trp1,ura3,rip1::KAN*^{R}	Stutz *et al*. (1997)
FSY38	*gle1-8* SL	**α**, *ade2,ade3,leu2,ura3,his3, ΔRIP1, gle1-8* (pFS652, URA3/ADE3/CEN)	this study; Stutz *et al*. (1997)
FSY57	*gle1-1* Rip1p low	**α**, *ade2,ade3,leu2,ura3,his3, ΔRIP1, gle1-1* (pFS724, LEU2/CEN)	Stutz *et al*. (1997)
FSY58	*gle1-1* Rip1p high	**α**, *ade2,ade3,leu2,ura3,his3, ΔRIP1, gle1-1* (pFS398, LEU2/CEN)	Stutz *et al*. (1997)
FSY216	*gle1-8*	**a**, *ade2,his3,leu2,trp1,ura3, gle1-8*	this study
FSY221	ProtA–RIP1	**a**, *ade2, his3, leu2,trp1,ura3, rip1::KAN*^{R} (pFS829, LEU2/CEN)	this study
FSY329	ProtA–RIP1-C66	**a**, *ade2, his3, leu2,trp1,ura3,rip1::KAN*^{R} (pFS923, LEU2/CEN)	this study
FSY195	GLE1 shuffle	**a**, *ade2, his3, leu2,trp1,ura3, gle1::HIS3* (pSW410, URA3/CEN)	this study, Murphy *et al.* (1996)
FSY201	GLE1 shuffle	**a**, *ade2, his3, leu2,trp1,ura3, gle1::HIS3, rip1::KAN*^{R} (pSW410, URA3/CEN)	this study, Murphy *et al*. (1996)
FSY292	*rss1-37 (gle1)*	**a**, *ade2, his3, leu2,trp1,ura3, gle1::HIS3* (pVDP29, LEU/CEN)	this study, Saavedra *et al*. (1997)
FSY251	ProtA–GLE1	**a**, *ade2, his3, leu2,trp1,ura3, gle1::HIS3* (pSW464, TRP1/CEN)	this study, Murphy *et al*. (1996)
FSY252	ProtA–GLE1 *ΔRIP1*	**a**, *ade2, his3, leu2,trp1,ura3, gle1::HIS3, rip1::KAN*^{R} (pSW464, TRP1/CEN)	this study, Murphy *et al*. (1996)
FSY297	GLE1–GFP	**a**, *ade2, his3, leu2,trp1,ura3, gle1::HIS3* (pFS1030, LEU2/CEN)	this study
FSY298	GLE1–GFP *ΔRIP1*	**a**, *ade2, his3, leu2,trp1,ura3, gle1::HIS3, rip1::KAN*^{R} (pFS1030, LEU2/CEN)	this study
CSY512	RAT8/DBP5 shuffle	**α**, *trp1Δ63,leu2Δ1,ura*3-52, his3*Δ*200, *rat8::HIS3* (pRAT8/DBP5, URA3/CEN)	Snay-Hodge *et al*. (1998)
CSY835	RAT8-GFP	**a**, *trp1Δ63,leu2Δ1,ura*3-52, his3*Δ*200, *rat8::HIS3* (pCS835, LEU2/CEN)	Snay-Hodge *et al*. (1998)
FSY342	ProtA–RAT8/DBP5	**α**, *trp1Δ63,leu2Δ1,ura*3-52, his3*Δ*200, *rat8::HIS3* (pCA5032, LEU2/CEN)	this study, Tseng *et al*. (1998), Snay-Hodge *et al*. (1998)
FSY398	W303 *GLE1–GFP*	**a**, *ade2, his3, leu2, trp1, ura3, GLE1-GFP-KAN*^{R}	this study
FSY399	*gle1-8-GFP*	**a**, *ade2, his3, leu2, trp1, ura3, gle1-8-GFP-KAN*^{R}	this study
CH1462		**α**, *ade2,ade3,leu2,ura3,his3*	Holm (1993), Stutz *et al*. (1997)
FSY249	*rss1-37 (gle1)*	**α**, *ade2,ade3,leu2,ura3,his3, rss1-37*	this study
FSY400	*rss1-37 RAT8-GFP*	**α**, *ade2,ade3,leu2,ura3,his3, rss1-37, RAT8/DBP5-GFP*	this study
FSY401	*rss1-37* pRAT8-GFP	**?**, *ade2,ade3,leu2,ura3,his3, rss1-37, rat8::HIS3* (pCS835, LEU2/CEN)	this study, Snay-Hodge *et al*. (1998)

Table III. Plasmids used in this study[a]

Name	Description		Source
pFS652		*RIP1 Hin*dIII genomic 3.5 kb fragment into *Sal*I of pCH1122 (URA3/CEN) with *Sal*I linkers	Stutz *et al*. (1997)
p366		YCP50-based vector in which URA3 was replaced with LEU2	Liao (1993)
pFS398	RIP1	*RIP1 Hin*dIII genomic 3.5 kb fragment inserted into the *Hin*dIII site of p366	Stutz *et al*.(1997)
pFS724	RIP1 low	*RIP1 Hin*dIII 1.9 kb PCR fragment inserted into the *Hin*dIII site of p366; contains 0.38 kb *RIP1* 5′-flanking sequences	Stutz *et al*. (1997)
pFS800		pFS398 with engineered *Sal*I site after the ATG	this study
pFS829	ProtA–RIP1	pFS800 with two IgG-binding domains (protein A) in the 5′ *Sal*I site	this study
pFS923	ProtA–RIP1-C66	pFS829 with a deletion of the FG-domain (codons 2–364)	this study
pSW464	ProtA–GLE1	*GLE1* with five IgG-binding domains inserted at the 5′ end (TRP1/CEN)	Murphy *et al*. (1996)
pCA5032	ProtA–RAT8	*DBP5/RAT8* with ProtA tag at the 3′ end in pRS315 (LEU2/CEN)	Tseng *et al*. (1998)
pFS952		*YMR255/GFD1* cloned in the *Eag*I site of YEp24 (URA3/2μ)	C.Cole laboratory (Dartmouth, VT)
pFS997		*RIP1 Hin*dIII genomic 3.5 kb fragment cloned in YEPLac112 (TRP1/2μ)	this study
pFS998		*GLE1* cloned as a *Sal*I fragment from pFS802 into YEPLac112	this study
pFS999		*RAT8* cloned as a *Sph*I-*Bam*HI fragment into YEPLac112	this study
pYGEX2T		Galactose-inducible GST fusion yeast expression vector (URA3/2μ)	P.Silver laboratory
pFS961	yGST–RIP1-C66	*RIP1* C-terminal codons 365–430 cloned as a *Bam*HI–*Hin*dIII fragment into pYGEX2T	this study
pFS802		*GLE1* gene cloned as a *Sal*I fragment into YCPLac111 (LEU2/CEN)	this study
pFS1029	GLE1 3′*Not*I	pFS802 with engineered *Not*I site upstream of *GLE1* stop codon	this study
pFS1030	GLE1-GFP	*GLE1 Sal*I fragment with GFP inserted into the engineered *Not*I site of pFS1029	this study
pCS835	RAT8-GFP	*RAT8-GFP* fusion cloned in YCPlac111 (LEU2/CEN)	Snay-Hodge *et al*. (1998)
pVDP29	prss1-37 (gle1)	*rss1-37* temperature-sensitive *GLE1* allele in YCP111 (LEU2/CEN)	Saavedra *et al*. (1997)
pFS410	GST–RIP1-FG	*RIP1* codons 121–230 cloned as an *Eco*RI–*Xho*I PCR fragment into pGex4T-1	this study
pFS507	GST–RIP1-C66	*RIP1* codons 364–430 cloned as an *Eco*RI–*Xho*I PCR fragment into pGex4T-1	this study
pFS883	GST–hCG1-C43	*hCG1* codons 380–423 cloned as an *Eco*RI–*Xho*I PCR fragment into pGex4T-1	this study
pFS955	GST–GFD1	*GFD1* coding region clones as an *Eco*RI–*Xho*I PCR fragment into pGex4T-1	this study
pFS956	GST–RAT8/DBP5	*RAT8/DBP5* coding region cloned as an *Eco*RI fragment into pGex4T-1	this study

[a]See Materials and methods for two-hybrid constructs.

*Hin*dIII site to the 3′ end of the two protein A moieties of pFS829 was ligated to a 1.5 kb *Xho*I–*Hin*dIII PCR fragment containing the last 66 codons of *RIP1* and 3′ sequences down to the natural *Hin*dIII site. The two PCR fragments were ligated through their *Xho*I ends and the product cloned back into the *Hin*dIII site of p366 (LEU2/CEN). ProtA–GLE1 (pSW464) and ProtA–RAT8 (pCA5032) have been described. The yGST–RIP1-C66 construct was obtained by cloning a 1.5 kb *Sal*I–*Hin*dIII PCR fragment comprising the last 66 codons of *RIP1* and 3′ sequences down to the natural *Hin*dIII site in-frame with the GST sequence of pYGEX2T (URA3/2μ) to generate pFS961.

The pGLE1-GFP plasmid (LEU2/CEN) was obtained by cloning the *GLE1* gene as a *Sal*I PCR fragment with 500 bp upstream and downstream sequences into YCPLac111 (LEU2/CEN) to generate pFS802. PCR was used to introduce a *Not*I site upstream of the *GLE1* stop codon in pFS802 to generate pFS1029. GFP (S65T) was cloned as a *Not*I PCR fragment into pFS1029 to generate pFS1030.

The high copy plasmid pFS997 was obtained by cloning the genomic 3.5 kb *RIP1 Hin*dIII fragment into YEpLac112 (TRP1/2μ). pFS998 was obtained by cloning the *GLE1 Sal*I fragment from pFS802 into YEpLac112. pFS999 was obtained by cloning the *RAT8/DBP5* gene as an *Sph*I–*Bam*HI fragment from pCS830 into the corresponding sites of YEPLac112. PFS952 was made by cloning the coding region of *YMR255w/GFD1* with 300 bp upstream and downstream sequences into vector YEp24 (URA3/2μ) as an *Eag*I PCR fragment (Cole Laboratory, Dartmouth, VT).

Two-hybrid LexA bait and prey cloning, strains and interaction assays

All baits were expressed as LexA fusions by cloning into vector pEG202 (HIS3/2μ); the prey constructs were obtained by cloning into pJG4-5 (TRP1/2μ) (Ausubel *et al*., 1994). The *GLE1* bait or prey constructs were obtained by inserting a *Bam*HI–*Sal*I or an *Eco*RI–*Sal*I PCR fragment corresponding to codons 257–538 of *GLE1* into pEG202 cut with *Bam*HI–*Xho*I or pJG4-5 cut with *Eco*RI–*Xho*I to generate pFS795 and pFS935, respectively. The RIP1-C66 bait and prey constructs were made by cloning a 500 bp *Eco*RI–*Sal*I PCR fragment corresponding to codons 365–430 and following 3′ sequences of *RIP1* into pEG202 or pJG4-5 cut with *Eco*RI–*Xho*I to generate pFS1031 and pFS1032. The RIP1-C38 bait and prey constructs were made by ligating a shorter *Eco*RI–*Sal*I fragment containing the last 38 codons of *RIP1* into pEG202 or pJG4-5 digested with *Eco*RI–*Xho*I to generate pFS1033 and pFS1034. The hCG1-C43 bait and prey constructs were obtained by inserting a 255 bp *Eco*RI–*Xho*I PCR fragment containing the last 43 codons followed by 3′ sequences into pEG202 and pJG4-5 cut with *Eco*RI–*Xho*I to generate pFS1035 and pFS1036. The hCG1 and hCG1-FG prey constructs were made by cloning *Eco*RI–*Xho*I PCR fragments of the whole coding region and codons 1–380, respectively, into pJG4-5 cut with *Eco*RI–*Xho*I to generate pFS1037 and pFS1038. The RIP1-FG bait construct pF5476 contains codons 121–130 of *Rip1* as an *Eco*RI–*Xho*I fragment in pEG202. The YMR255/GFD1 prey construct pFS1039 contains the whole coding region as an *Eco*RI–*Xho*I PCR fragment in pJG4-5 *Eco*RI–*Xho*I. The DBP5/RAT8 prey plasmid pFS1040 contains the whole coding region as an *Eco*RI PCR fragment in pGJ4-5 *Eco*RI. The CRM1 and Rev bait as well as the Rev and RIP1-FG prey constructs have been described (Stutz *et al*., 1995; Neville *et al*., 1997).

Strain EGY48 (α, *trp1 ura3 leu2*::plexop6-LEU2) containing the LacZ reporter pSH18-34 on a URA3/2μ plasmid was transformed with the prey constructs. Strain RFY206 (a, *his3 leu2 ura3 trp1 lys2*) and containing pSH18-34 was transformed with the bait constructs. Two-hybrid interactions were examined by mating followed by replica-plating of the diploids on X-Gal indicator plates containing galactose as described earlier (Stutz *et al*., 1995).

In vivo protein labeling

Yeast cultures grown at 25°C or shifted to 42°C were labelled with [^{35}S]methionine as described (Stutz *et al*., 1997). Total cell lysates were fractionated on a 10% SDS–polyacrylamide gel. Gels were dried and autoradiographed.

High copy suppressor screen

The *gle1-8* mutant allele had been identified earlier in a screen for mutants synthetically lethal with a *RIP1* deletion. The mutant allele was amplified by PCR (High Fidelity Expand PCR, Boehringer MA) from genomic DNA as a *Sal*I fragment containing 500 bp on both sides of the coding region and cloned into YCPLac111 (LEU2/CEN) to generate pFS824. pFS824 was confirmed to contain the *gle1-8* mutation(s) by testing its synthetic lethality with a *RIP1* deletion. The mutations in the *gle1-8* allele were identified by sequencing both strands of overlapping PCR fragments spanning the whole wild-type or mutant gene. Comparison of the two sequences identified three mutations, two of which induced amino acid changes (T21A and E340K).

To construct the starting strain for the high copy suppressor screen, the mutant *gle1-8* allele was integrated into the genome of a W303 wild-type strain at the *GLE1* locus by the pop-in/out replacement method to generate FSY216. Briefly, the *Sal*I insert of pFS824 was subcloned into the *Xho*I site of the yeast integrating plasmid pRS406 (URA3; Stratagene) to generate pFS845. pFS845 was linearized with *Xho*I and transformed into W303. URA$^+$ colonies were collected, grown overnight in YEPD medium and plated on 5-FOA. 5-FOA$^+$ colonies were replica-plated to YEPD containing 7.5 mg/l of the vital dye erythrosin B (Sigma) and incubated at 37°C. The strains with the *gle1-8* ts allele were identified based on slow growth and purple colour.

The *gle1-8* high copy suppressors were identified by transforming strain FSY216 with a yeast genomic library cloned in YEp13 (LEU2/2μ). A total of 5×10^4 transformants were grown at 25°C on SD-Leu plates, collected and replated on SD-Leu plates at 37°C. Library plasmids were rescued from colonies growing at 37°C and retransformed into FSY216 to verify the suppressor phenotype. The rescuing plasmids were sequenced from both sides of the insert. Individual ORFs were subcloned into YEpLac112 vector (TRP1/2μ) as described above.

Growth curves were established by diluting exponentially growing cultures to an $OD_{600} = 0.05$ (~5×10^5 cells/ml). The diluted cultures were incubated for 2 h at 25°C and then shifted to 37°C. Growth rates were followed by measuring OD_{600} at various time intervals over 24 h.

Western blot analysis

Protein extracts and Western blots were performed as described (Stutz *et al*., 1997). The anti-Gle1p and anti-Rna15p antibodies were used at 1:2000 and 1:15 000 dilutions, respectively.

In vitro translation

[^{35}S]Methionine-labelled full-length Gle1p and Gle1p C-terminus were obtained by coupled T7 transcription–translation in reticulocyte lysates (TnT kit, Promega). T7 templates were generated by PCR. The template for full-length Gle1p was obtained by amplifying wild-type *GLE1* with the 5′ primer OFS296 5′-GGGCGAAATTAATACGACTCACTAT-AGGGACACCATGAGATTTGTGTTCGATGAGGTTTT-3′, containing the T7 RNA polymerase promoter and sequences complementary to the 5′ end of the *GLE1* coding region, and the 3′ primer OFS138 5′-CGTATTTTCTGCCATCCCTTGATATCGAGCCG-3′ complementary to a region of *GLE1* downstream of the stop codon. The template for the Gle1p C-terminus was generated with the 5′ primer OFS385 5′-GGGCGAAATTAATACGACTCACTATAGGGACACCATGGACA-AAATTGCTCAAATAAAGC-3′, containing the T7 promoter and sequences complementary to *GLE1* starting from codon 257, and with the OFS138 3′ primer. A 2 μg aliquot of each T7 PCR template was used per 25 μl transcription–translation reaction.

GST fusions and in vitro binding assay

The constructs used to produce GST fusions in *E.coli* were obtained by cloning PCR fragments into vector pGex-4T-1 (Pharmacia Biotech). GST–RIP1-FG and GST–RIP1-C66 were made by inserting *Eco*RI–*Xho*I fragments, corresponding to codons 121–230 and 364–430 of *RIP1*, respectively, into pGex-4T-1 *Eco*RI–*Xho*I to generate pFS410 and pFS507. GST–hCG1-C43 was obtained by inserting a 255 bp *Eco*RI–*Xho*I PCR fragment corresponding to the last 43 codons and 3′-untranslated sequences of hCG1 into pGex-4T-1 *Eco*RI–*Xho*I to generate pFS883. The complete coding sequences of *DBP5/RAT8* and *YMR255w/GFD1* were amplified as *Eco*RI and *Eco*RI–*Xho*I fragments, respectively, and cloned into pGex4T-1 cut with the corresponding enzymes to generate pFS955 and pFS956.

The GST fusion constructs were transformed into *E.coli* strain BL21(DE3) and fusion protein synthesis was induced overnight at 16°C in the presence of 0.5 mM isopropyl-β-D-thiogalactopyranoside (IPTG). After cell lysis, GST fusions were affinity purified on glutathione–agarose beads (Pharmacia) as described by the manufacturer. *In vitro* binding reactions contained 10 μg of GST fusion protein immobilized on 25 μl of packed glutathione–agarose beads and 1/10 of an *in vitro* transcription–translation reaction (2.5 μl) in 100 μl of universal binding buffer [20 mM HEPES pH 7, 10% glycerol, 0.1% bovine serum albumin (BSA), 0.1% Tween, 100 mM KOAc, 2 mM MgOAc, 5mM β-mercaptoethanol and 1 tablet/50 ml of protease inhibitors (Boehringer)]. Binding reactions were incubated for 1 h at 4°C on a turning wheel and washed three times with 500 μl of binding buffer. The beads were resuspended in 20 μl of 2× sample buffer, boiled and 1/4 of the binding reaction (10 μl) was fractionated on 10% polyacrylamide gels. To evaluate binding efficiency, 1/4 of the *in vitro* translated protein input (0.6 μl) was loaded in parallel. After Coomassie Blue staining, gels were dried and autoradiographed.

In situ hybridization

Strain FSY292 (*rss1-37*) was obtained by transforming the *GLE1* shuffle strain FSY197 with pVDP29 (p*rss1-37*, LEU2/CEN) followed by selection on 5-FOA. Strains FSY57 (*gle1-1*, Rip1p low) and FSY58 (*gle1-1*, Rip1p normal) have been described (Stutz *et al*., 1997). Yeast strains were grown to $OD_{600} = 0.5$ at 25°C. Half of each culture was shifted to 37°C by the addition of 1 vol. of medium pre-heated to 49°C and incubated for 30 min at 37°C. Cells were fixed and processed for *in situ* hybridization with digoxigenin-labelled oligo(dT) probes on multi-well slides as described (Neville *et al*., 1997). Pictures were taken

on a Zeiss axioplan 2 fluorescence microscope equipped with a cooled CCD camera and 100× and 63× objective lenses. Identical exposure times were used for comparable images, and composites were prepared using Adobe Photoshop.

Immunoelectron microscopy localizations

The ProtA–Gle1p strains FSY251 and FSY252 were obtained by transforming pSW464 (Murphy and Wente, 1996) into the GLE1 shuffle strains FSY195 or FSY201 followed by selection on 5-FOA. The ProtA–Rat8p/Dbp5p strain FSY342 was obtained by transforming pCA5032 into the RAT8/DBP5 shuffle strain CSY512 followed by selection on 5-FOA. The ProtA–Rip1p strains FSY221 and FSY329 were obtained by transforming pFS829 and pFS923 into FSY17 (W303 *ΔRIP1*).

The localization of the ProtA–fusions was determined by using a pre-embedding labelling protocol essentially as described (Fahrenkrog *et al*., 1998). Briefly, the cells were spheroplasted, washed and treated with Triton X-100. Triton-extracted cells were washed, resuspended in 100 µl of anti-protein A antibody labelled with 8 nm colloidal gold and incubated at 30°C. The cells were then washed, fixed, dehydrated, Epon embedded and prepared for electron microscopy as described. The pre-embedding labelling conditions were adapted for each strain analysed. ProtA–Rip1p in *ΔRIP1*: 15 min zymolyase digest, 0.05% Triton X-100 extraction, 2.5 h antibody labelling; ProtA–Rip1p-C66 in *ΔRIP1*: 15 min zymolyase digest, 0.025% Triton X-100 extraction, 2.5 h labelling; ProtA–Rip1p in *ΔRIP1 at* 42°C: 10 min heat shock, 10 min zymolyase digest, 0.025% Triton X-100, 1 h labelling. ProtA–Gle1p in *ΔGLE1* or *ΔGLE1ΔRIP1* background: 20 min zymolyase digest, 0.05% Triton X-100, 2.5 h labelling; ProtA–Rat8p in *ΔRAT8* background: 15 min zymolyase, 0.025% Triton, 2.5 h labelling.

In vivo localizations

Strains FSY297 (*ΔGLE1* pGLE1-GFP) and FSY298 (*ΔGLE1ΔRIP1* pGLE1-GFP) were obtained by transforming pFS1030 into the *GLE1* shuffle strains FSY195 (*gle1::HIS3*, pGLE1 URA/CEN) or FSY201 (*gle1::HIS3, rip1::KAN*^{R} pGLE1 URA/CEN), followed by selection on 5-FOA. Cells were transformed with a pRSADE2 plasmid to minimize vacuolar fluorescence. The *gle1-8* allele in FSY216 and the wild-type *GLE1* gene in W303 were chromosomally tagged with GFP using the pFA6a-GFP(S65T)-KanMX6 module as described (Longtine *et al*., 1998) to generate FSY399 and FSY398, respectively. These strains were transformed with high copy plasmids and pRSADE2. The temperature-sensitive *rss1-37 (gle1)* strain FSY249 was obtained by replacing wild-type *GLE1* by the *rss1-37* mutant allele (Saavedra *et al*., 1997) in strain CH1462 (Holm, 1993); the strategy was the same as the one used to generate FSY216 (see above). The *rss1-37* allele of strain FSY249 was tagged with GFP using the pFA6a-GFP(S65T)-kanMX6 module (Longtine *et al*., 1998) to generate FSY400; FSY249 was also crossed with strain CSY835 (*rat8/dbp5*::HIS3, pCS835) (Snay-Hodge *et al*., 1998) to generate the haploid strain FSY401, a *rss1-37 rat8/dbp5::HIS3* double mutant strain expressing Rat8p/Dbp5p–GFP from plasmid pCS835 (LEU2/CEN). All the strains were grown in selective or SD complete medium to early logarithmic phase, shifted for various times to 37°C, spun for a short time and examined directly under a Zeiss axioplan 2 fluorescence microscope equipped with a 100× objective lens and a cooled CCD camera (Kappa). Pictures were taken as described for *in situ* hybridizations.

Acknowledgements

We are grateful to Chuck Cole for valuable discussions and for sharing data prior to publication. We thank Chuck Cole, Tien-Hsien Chang, Pamela Silver and Susan Wente for plasmids and yeast strains, Laura Davis and Lionel Minvielle-Sebastia for antibodies, and Lut Van Laer and the UK HGMP resource centre for the hCG1 cDNA. We also thank Elisa Izaurralde and Hildur V.Colot for critical reading of the manuscript. We acknowledge Verena Müller for technical support, and members of the Microbiology Institute for their help. B.F. was supported by the M.E.Mueller Foundation of Switzerland and by an HFSP grant awarded to Ueli Aebi. These studies were supported by a research grant (No. 049135.96/1) from the Swiss National Science Foundation to F.S.

References

Ausubel,F.M., Brent,R., Kingston,R.E., Moore,D.D., Seidman,J.G., Smith,J.A. and Struhl,K. (1994) *Current Protocols in Molecular Biology*. J.Wiley & Sons and Greene Publishing Associates.

Belgareh,N., Snay-Hodge,C., Pasteau,F., Dagher,S., Cole,C.N. and Doye,V. (1998) Functional characterization of a Nup159p-containing nuclear pore subcomplex. *Mol. Biol. Cell*, **9**, 3475–3492.

Bogerd,H.P., Fridell,R.A., Madore,S. and Cullen,B.R. (1995) Identification of a novel cellular cofactor for the Rev/Rex class of retroviral regulatory proteins. *Cell*, **82**, 485–494.

Dahlberg,J.E. and Lund,E. (1998) Functions of the GTPase Ran in RNA export from the nucleus. *Curr. Opin. Cell Biol.*, **10**, 400–408.

de Castillia,C.S. and Rout,M.P. (1999) TAPping into transport. *Nature Cell Biol.*, **1**, 31–33.

Del Priore,V., Snay,C.A., Bahr,A. and Cole,C.N. (1996) The product of the *Saccharomyces cerevisiae RSS1* gene, identified as a high-copy suppressor of the *rat7-1* temperature-sensitive allele of the *RAT7/NUP159* nucleoporin, is required for efficient mRNA export. *Mol. Biol. Cell*, **7**, 1601–1621.

Del Priore,V., Heath,C.V., Snay,C.A., MacMillan,A., Gorsch,L.C., Dagher,S. and Cole,C.N. (1997) A structure/function analysis of Rat7p/Nup159p, an essential nucleoporin of *Saccharomyces cerevisiae*. *J. Cell Sci.*, **110**, 2897–2999.

Doye,V. and Hurt,E. (1997) From nucleoporins to nuclear pore complexes. *Curr. Opin. Cell Biol.*, **9**, 401–411.

Fabre,E. and Hurt,E. (1997) Yeast genetics to dissect the nuclear pore complex and nucleocytoplasmic trafficking. *Annu. Rev. Genet.*, **31**, 277–313.

Fahrenkrog,B., Hurt,E.C., Aebi,U. and Panté,N. (1998) Molecular architecture of the yeast nuclear pore complex: localization of Nsp1p subcomplexes. *J. Cell Biol.*, **143**, 577–588.

Farjot,G., Sergeant,A. and Mikaélian,I. (1999) A new nucleoporin-like protein interacts with both HIV-1 Rev nuclear export signal and CRM-1. *J. Biol. Chem.*, **274**, 17309–17317.

Floer,M. and Blobel,G. (1999) Putative reaction intermediates in Crm1-mediated nuclear protein export. *J. Biol. Chem.*, **274**, 16279–16286.

Fontoura,B.M.A., Blobel,G. and Matunis,M.J. (1999) A conserved biogenesis pathway for nucleoporins: proteolytic processing of a 186-kilodalton precursor generates Nup98 and the novel nucleoporin, Nup96. *J. Cell Biol.*, **144**, 1097–1112.

Fritz,C.C., Zapp,M.L. and Green,M.R. (1995) A human nucleoporin-like protein that specifically interacts with HIV Rev. *Nature*, **376**, 530–533.

Görlich,D. (1998) Transport into and out of the cell nucleus. *EMBO J.*, **17**, 2721–2727.

Grüter,P., Tabernero,C., von Kobbe,C., Schmitt,C., Saavedra,C., Bachi,A., Wilm,M., Felber,B.K. and Izaurralde,E. (1998) TAP, the human homolog of Mex67p, mediates CTE-dependent RNA export from the nucleus. *Mol. Cell*, **1**, 649–659.

Hodge,C.A., Colot,H.V., Stafford,P. and Cole,C.N. (1999) Rat8p/Dbp5 is a shuttling transport factor that interacts with Rat7p/Nup159p and Gle1p and suppresses the mRNA export defect of *xpo1-1* cells. *EMBO J.*, **18**, 5778–5788.

Holm,C. (1993) A functional approach to identifying yeast homologs of genes from other species. *Methods*, **5**, 102–109.

Hurwitz,M.E., Strambio-de-Castillia,C. and Blobel,G. (1998) Two yeast nuclear pore complex proteins involved in mRNA export form a cytoplasmically oriented subcomplex. *Proc. Natl Acad. Sci. USA*, **95**, 11241–11245.

Izaurralde,E. and Adam,S. (1998) Transport of macromolecules between the nucleus and the cytoplasm. *RNA*, **4**, 351–364.

Izaurralde,E., Kutay,U., von Kobbe,C., Mattaj,I.W. and Gorlich,D. (1997) The asymmetric distribution of the constituents of the Ran system is essential for transport into and out of the nucleus. *EMBO J.*, **16**, 6535–6547.

Katahira,J., Strässer,K., Podtelejnikov,A., Mann,M., Jung,J.U. and Hurt,E. (1999) The Mex67p-mediated nuclear mRNA export pathway is conserved from yeast to human. *EMBO J.*, **18**, 2593–2609.

Kraemer,D.M., Strambio-de-Castillia,C., Blobel,G. and Rout,M.P. (1995) The essential yeast nucleoporin NUP159 is located on the cytoplasmic side of the nuclear pore complex and serves in karyopherin-mediated binding of transport substrate. *J. Biol. Chem.*, **270**, 19017–19021.

Liao,X.C., Tang,J. and Rosbash,M. (1993) An enhancer screen identifies a gene that encodes the yeast U1 snRNP A protein: implications for snRNP protein function in pre-mRNA splicing. *Genes Dev.*, **7**, 419–428.

Longtine,M.S., McKenzie,A., Demarini,D.J., Shah,N.G., Wach,A., Brachat,A., Philippsen,P. and Pringle,J.R. (1998) Additional modules for versatile and economical PCR-based gene deletion and modification in *Saccharomyces cerevisiae*. *Yeast*, **14**, 953–961.

Mattaj,I.W. and Englmeier,L. (1998) Nucleocytoplasmic transport: the soluble phase. *Annu. Rev. Biochem.*, **67**, 265–306.
Murphy,R. and Wente,S.R. (1996) An RNA-export mediator with an essential nuclear export signal. *Nature*, **383**, 357–360.
Nakielny,S., Fischer,U., Michael,W.M. and Dreyfuss,G. (1997) RNA transport. *Annu. Rev. Neurosci.*, **20**, 269–301.
Nakielny,S., Shaikh,S., Burke,B. and Dreyfuss,G. (1999) Nup153 is an M9-containing mobile nucleoporin with a novel Ran-binding domain. *EMBO J.*, **18**, 1982–1995.
Neville,M. and Rosbash,M. (1999) The NES–Crm1p export pathway is not a major mRNA export route in *Saccharomyces cerevisiae*. *EMBO J.*, **18**, 3746–3756.
Neville,M., Stutz,F., Lee,L., Davis,L.I. and Rosbash,M. (1997) Evidence that the importin-beta family member Crm1p bridges the interaction between Rev and the nuclear pore complex during nuclear export in *S.cerevisiae*. *Curr. Biol.*, **7**, 767–775.
Noble,S.M. and Guthrie,C. (1996) Identification of novel genes required for yeast pre-mRNA splicing by means of cold-sensitive mutations. *Genetics*, **143**, 67–80.
Pollard,V.W. and Malim,M.H. (1998) The HIV-1 Rev protein. *Annu. Rev. Microbiol.*, **52**, 491–532.
Saavedra,C.A., Hammell,C.M., Heath,C.V. and Cole,C.N. (1997) Export of heat shock mRNAs following stress in *Saccharomyces cerevisiae* employs a distinct pathway defined by Rip1p and also requires a subset of factors essential for export of poly(A)$^+$ mRNA. *Genes Dev.*, **11**, 2845–2856.
Santos-Rosa,H., Moreno,H., Simos,G., Segref,A., Fahrenkrog,B., Panté,N. and Hurt,E. (1998) Nuclear mRNA export requires complex formation between Mex67p and Mtr2p at the nuclear pores. *Mol. Cell. Biol.*, **18**, 6826–6838.
Schmitt,C. *et al*. (1999) Dbp5p, a DEAD box-protein required for mRNA export, is recruited to the cytolasmic fibrils of nuclear pore complex via a conserved interaction with CAN/Nup159p. *EMBO J.*, **18**, 4332–4347.
Siniossoglou,S., Wimmer,C., Rieger,M., Doye,V., Tekotte,H., Weise,C., Emig,S., Segref,A. and Hurt,E.C. (1996) A novel complex of nucleoporins, which includes Sec13p and a Sec13p homolog, is essential for normal nuclear pores. *Cell*, **84**, 265–275.
Snay-Hodge,C.A., Colot,H.V., Goldstein,A.L. and Cole,C.N. (1998) Dbp5p/Rat8p is a yeast nuclear pore-associated DEAD-box protein essential for RNA export. *EMBO J.*, **17**, 2663–2676.
Stade,K., Ford,C.S., Guthrie,C. and Weis,K. (1997) Exportin 1 (Crm1p) is an essential nuclear export factor. *Cell*, **90**, 1041–1050.
Stoffler,D., Fahrenkrog,B. and Aebi,U. (1999) The nuclear pore complex: from molecular architecture to functional dynamics. *Curr. Opin. Cell Biol.*, **11**, 391–401.
Stutz,F. and Rosbash,M. (1998) Nuclear RNA export. *Genes Dev.*, **12**, 3303–3319.
Stutz,F., Neville,M. and Rosbash,M. (1995) Identification of a novel nuclear pore-associated protein as a functional target of the HIV-1 Rev protein in yeast. *Cell*, **82**, 495–506.
Stutz,F., Kantor,J., Zhang,D., McCarthy,T., Neville,M. and Rosbash,M. (1997) The yeast nucleoporin Rip1p contributes to multiple export pathways with no essential role for its FG-repeat region. *Genes Dev.*, **11**, 2857–2868.
Teixeira,M.T., Siniossoglou,S., Podtelejnikov,S., Bénichou,J.C., Mann,M., Dujon,B., Hurt,E. and Fabre,E. (1997) Two functionally distinct domains generated by *in vivo* cleavage of Nup145p: a novel biogenesis pathway for nucleoporins. *EMBO J.*, **16**, 5086–5097.
Tseng,S.I., Weaver,P.L., Liu,Y., Hitomi,M., Tartakoff,A.M. and Chang,T.H. (1998) Dbp5p, a cytosolic RNA helicase, is required for poly(A)$^+$ RNA export. *EMBO J.*, **17**, 2651–2662.
Van Laer,L. *et al*. (1997) Refined mapping of a gene for autosomal dominant progressive sensorineural hearing loss (DFNA5) to a 2-cM region, and exclusion of a candidate gene that is expressed in the cochlea. *Eur. J. Hum. Genet.*, **5**, 397–405.
Watkins,J.L., Murphy,R., Emtage,J.L. and Wente,S.R. (1998) The human homologue of *Saccharomyces cerevisiae* Gle1p is required for poly(A)$^+$ RNA export. *Proc. Natl Acad. Sci. USA*, **95**, 6779–6784.
Zolotukhin,A.S. and Felber,B.K. (1999) Nucleoporins Nup98 and Nup214 participate in nuclear export of human immunodeficiency virus type 1 Rev. *J. Virol.*, **73**, 120–127.

Received June 21, 1999; revised and accepted August 31, 1999